

ANALYTICAL METHOD DEVELOPMENT FOR CYANIDE ANTIDOTES AND
CHARACTERIZATION OF A NEW FORMULATION OF DIMETHYL TRISULFIDE

A Thesis

Presented to

The Faculty of the Department of Chemistry

Sam Houston State University

In Partial Fulfillment

of the Requirements for the Degree of

Master of Science

by

Chathuranga Chinthana Hewa Rahinduwage

August, 2017

ANALYTICAL METHOD DEVELOPMENT FOR CYANIDE ANTIDOTES AND
CHARACTERIZATION OF A NEW FORMULATION OF DIMETHYL TRISULFIDE

by

Chathuranga Chinthana Hewa Rahinduwage

APPROVED:

Ilona Petrikovics, PhD
Thesis Director

Donovan C. Haines, PhD
Committee Member

David E. Thompson, PhD
Committee Member

John B. Pascarella, PhD
Dean, College of Science and Engineering
Technology

DEDICATION

I would like to dedicate my thesis to:

- My parents who gave me life
- My beautiful and loving wife, Surige Heshani Chamalka, who makes life so easy and beautiful
- My wonderful research supervisor, Dr. Ilona Petrikovics, whom I consider as my academic mother
- All the teachers I met throughout my entire life who enriched my knowledge, character and beliefs

ABSTRACT

Hewa Rahinduwage, Chathuranga Chinthana, *Analytical method development for cyanide antidotes and characterization of a new formulation of dimethyl trisulfide*. Master of Science (Chemistry), August, 2017, Sam Houston State University, Huntsville, Texas.

Cyanide (CN) is one of the most highlighted toxic compounds. It inhibits the cytochrome c oxidase enzyme, which catalyzes oxygen utilization in cells. As the brain and the heart are the main oxygen consumers, the effects of CN are more prominent on these organs. CN is converted into the less toxic thiocyanate in the presence of a sulfur donor, such as DMTS or thiosulfate (TS). In-house analytical methods were developed to determine CN, TS and nitrite (NT) concentrations by ion chromatograph (IC). Two different formulations for DMTS have been prepared for intramuscular (IM) administration. Formulation 1 (DMTS-F1) is a dispersion of DMTS in 15% aqueous polyoxyethylenesorbitan monooleate (poly80) solution. Formulation 2 (DMTS-F2) is a dispersion of DMTS in a mixture of poly80 and sorbitan monooleate (span80) (1:3 w/w). The concentrations of DMTS in F1 is 50 mg/mL and in F2 is 400 mg/mL. The Blood Brain Barrier (BBB) penetration by the two formulated DMTS structures were studied in a BBB model, Parallel Artificial Membrane Permeability Assay (PAMPA). The PAMPA system has two compartments to model the brain side and the blood vessel side of the BBB. Those compartments are separated with a porcine brain lipid-impregnated membrane. The antidote concentrations in the PAMPA samples were determined by HPLC with UV detection. In the first 30 minutes DMTS-F1 showed much higher speed in traveling from the blood to the brain side of the PAMPA. However, after 30 minutes DMTS-F2 showed much higher travel speed to the brain side. The size distribution stability of the two formulations were measured using a dynamic light scattering (DLS) instrument (Zetasizer). For quality measurements, this technique requires an estimate of the viscosity of the liquid. The viscosity of 2.32 cP for DMTS-F1 and 511.00 cP for DMTS-F2 were measured by a dropping ball viscometer. Size distribution studies suggest that the DMTS-F1 stored at 4 °C provides much more stable droplet size.

KEY WORDS: Cyanide, Antidote Formulations, Dimethyl Trisulfide, Blood Brain Barrier Penetration, Size Distribution

ACKNOWLEDGEMENTS

The biggest support behind my research work was the guidance and the support of my supervisor Dr. Ilona Petrikovics, Dr. David Thompson, Dr. Donovan Haines, Dr. Lorand Kiss, Dr. Afshin Ebrahimpour and Dr. Marton Kiss. I am sincerely thankful to all of them for their valuable contributions. Also, I am grateful to the other research members in the Dr. Petrikovics' lab for their support and company. I appreciate the financial support given by the Robert A. Welch Foundation at Sam Houston State University, by the College of Science and Engineering Technology at Sam Houston State University and the United States Army Medical Research Institute of Chemical Defense. Finally, I would like to thank my friends, teachers, my wife and my parents for the strengths they have enriched into me to achieve the goals of my higher education.

TABLE OF CONTENTS

	Page
DEDICATION	iii
ABSTRACT	iv
ACKNOWLEDGEMENTS	v
TABLE OF CONTENTS.....	vi
LIST OF TABLES	viii
LIST OF FIGURES	ix
CHAPTER	
I INTRODUCTION	1
Toxicity of Cyanide (CN)	1
Current Cyanide Antidotes and their Drawbacks	3
Dimethyl Trisulfide (DMTS).....	4
Blood Brain Barrier (BBB).....	5
Parallel Artificial Membrane Permeability Assay (PAMPA).....	5
Particle Size Determination and the DLS Instrument.....	7
II MATERIALS AND METHODS.....	9
Chemicals.....	9
Instruments.....	10
Methods.....	10
III RESULTS	26
Preparation of two DMTS Formulations based on Known Methods	26
Analytical Method Development for CN by Ion Chromatography (IC).....	28

Analytical Method Development for NT quantitation using IC	33
Analytical Method Development to Determine DMTS in the PAMPA System Using HPLC-UV.....	37
Calibration curve 1 and the PAMPA analysis of DMTS-F1	37
Calibration curve 2 and comparison of the BBB penetration of two DMTS formulations	41
BBB Penetration Determination of DMTS in Two Formulations by the PAMPA System.....	44
Viscosity Determination of the Two Dispersants of the DMTS Formulations	50
Droplet Size Distribution of DMTS-F1 Using DLS Instrument.....	52
Analytical Method Development to Determine DMTS in Blood Samples, Collected During Pharmacokinetics Studies, by Using HPLC.....	57
IV CONCLUSION.....	61
Analytical Method Development for CN, TS and NT by Using IC	61
Analytical Method Development for DMTS detection by HPLC-UV	61
Viscosity and Droplet Size Distribution Kinetics of DMTS-F1 and DMTS-F2 ..	62
BBB Penetration of DMTS-F1 and DMTS-F2.....	62
Pharmacokinetics Study.....	62
Future Recommendations	63
REFERENCES	64
APPENDIX.....	70
VITA.....	71

LIST OF TABLES

Table		Page
1	Instruments Used for the Research.	10
2	Particle Size Distribution of the DMTS-F1 Right After Preparation.	26
3	Viscosity Calculation for DMTS-F1 and DMTS-F2	51
4	Average Droplet Size Results for the DMTS-F1 Samples Stored at 4 °C, 25 °C and 37 °C for One Hour After the Preparation.....	53

LIST OF FIGURES

Figure	Page
1 Dissociation of HCN.....	2
2 PAMPA Sandwiched Plates.....	6
3 PAMPA Membranes on the Bottom of the Acceptor Plate.....	7
4 PAMPA Donor Plate.....	7
5 Block Diagram for the DLS Instrument, Zetasizer Nano ZS.....	8
6 Preparation of the DMTS-F1.	11
7 Preparation of DMTS-F2.	11
8 Experimental Setup to Determine the Effect of poly80 on DMTS Permeability.	17
9 Effect of Poly80 in the Acceptor Wells on Permeability.....	18
10 Effect of the Stirrers on DMTS Permeability.	19
11 Placing Stirrers (0, 1, 2) in the Acceptor and the Donor Wells.	19
12 Dropping Ball Viscometer with the Travelling Metal Ball.	21
13 Flow Chart for the Pharmacokinetic Study.....	25
14 Droplet Size Distribution of DMTS-F1 Right After Preparation.	27
15 Droplet Size Distribution of the Original DMTS-F2 Received from SwRI.	27
16 Droplet Size Distribution of the Freshly Prepared DMTS-F2.....	28
17 Comparison of the Droplet Size Distribution of the Freshly Prepared DMTS- F2 in Our Lab vs. the Original DMTS-F2 Sample Prepared by SwRI.	28
18 Ion Chromatogram for the CN Blank (0 mg/ mL CN).	29
19 Ion Chromatogram for 0.1 mg/mL CN.	29

20	CN Calibration Curve Measured by IC.	30
21	Ion Chromatogram for the TS Blank (0 mg/ mL).....	31
22	Ion Chromatogram for TS (0.005 mg/ mL).	32
23	Ion Chromatogram for TS (0.05 mg/ mL).	32
24	Peak Area vs. TS Concentration.	33
25	Ion Chromatogram for the NT Blank (0.000 mg/ mL NT).....	34
26	Ion Chromatogram for NT (0.100 mg/ mL).....	34
27	Ion Chromatogram for NT (0.800 mg/ mL).....	35
28	Calibration Curve for NT Using IC.	36
29	Characteristic HPLC-UV Spectrum Observed for DMTS.....	37
30	Calibration Curve (1) Observed for DMTS.	38
31	DMTS Concentration Variation in the Acceptor Wells.....	39
32	DMTS Concentration Variation in the Donor Wells.	40
33	Membrane Retention for DMTS-F1.	40
34	Calibration Curve (2) for DMTS.	41
35	DMTS Calibration Curve (2a) for Concentrations below 0.05 mg/mL.....	43
36	DMTS Calibration Curve (2b) for Concentrations Above 0.05 mg/mL.....	44
37	Overlay of DMTS Concentrations in the Acceptor Phase of the PAMPA system for DMTS-F1 and DMTS-F2.....	45
38	DMTS Concentration from DMTS-F1 and DMTS-F2 in the Donor Phase of the PAMPA.....	45
39	Membrane Retention from DMTS-F1 and DMTS-F2 in the Acceptor Phase of the PAMPA System.	46

40	Effect of poly80 to the DMTS Concentration in the Acceptor Phase.....	47
41	Effect of poly80 to the DMTS Concentration in the Donor Phase.	48
42	DMTS Concentration in the Acceptor Phase with Different Number of Stirrers.	49
43	DMTS Concentration in the Donor Phase with Different Number of Stirrers.	50
44	Distributing the DMTS-F1 Stocks Solution to Three Different Temperature Groups.....	53
45	Size Distribution of the DMTS-F1 One Hour After Preparation.....	54
46	Major Droplet Size and the Percentage Variation with Sampling Time for DMTS-F1 at 4°C.	55
47	Major Droplet Size and the Percentage Variation with Sampling Time for DMTS-F1 at 25°C.	56
48	Major Droplet Size and the Percentage Variation with Sampling Time for DMTS-F1 at 37°C.	56
49	Calibration Curve for DMTS in Blood.	58
50	DMTS Concentration in Rat Blood for DMTS-F1.	59
51	DMTS Concentration in Rat Blood for DMTS-F2.	60

CHAPTER I

INTRODUCTION

Toxicity of Cyanide (CN)

There are two major types of cellular respiration pathways, the aerobic and the anaerobic pathway. In eukaryotes, the aerobic pathway is the predominant respiration form, which can be subdivided into three steps: glycolysis, the Krebs cycle and the electron transfer chain. The glucose molecule is oxidized through this process to provide adenosine triphosphate (ATP). This process is powered by the reduction of oxygen at the final step of the electron transfer chain.¹ Cytochrome c oxidase is the terminal oxidase enzyme of the electron transfer chain. The toxic effects of CN are attributed to the inhibition of the aerobic respiratory pathway by binding and inhibiting this enzyme. CN has strong affinity to cytochrome c oxidase. A two-step mechanism was proposed to explain this inhibition. First, CN binds to cytochrome c oxidase, then it forms a stable coordination metal complex via the trivalent Fe^{3+} metal center of the enzyme.^{2,3} Once CN binds to the enzyme, the mitochondrial electron transport is interrupted. This is the reason for the resulting histotoxic hypoxia, the inability to utilize oxygen for cellular respiration. The heart and the brain are the two organs that require the most oxygen. Consequently, they are most sensitive to CN intoxication. As a result, the anaerobic metabolic pathway comes into action to provide the required energy to the cells. Anaerobic respiration also uses glucose as its substrate, but it leads to lactic acid production. The lactic acid tends to accumulate inside the cell and high levels of it can damage the cellular organelles. This condition is called lactic acidosis.¹

HCN is a weak acid with a pK_a of 9.2. At physiological pH of 7.4, the predominant form is HCN (Figure 1). It is a small molecule and it can readily cross the membranes of the cells.^{4,5}

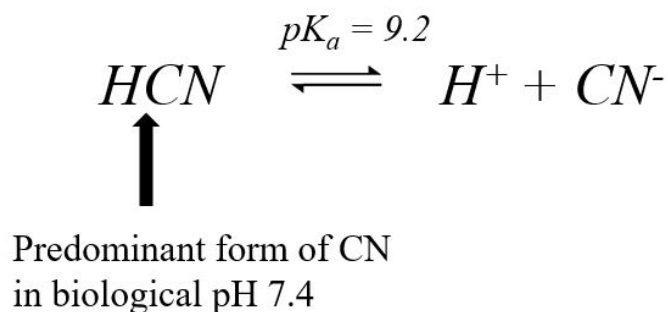


Figure 1. Dissociation of HCN. HCN is a weak acid which dissociates into H^+ and CN^- in aqueous solutions. The ratio of the non-ionized form to ionized form depends on the pH of the media.

CN is used in industries such as gold mining, textile manufacturing and electroplating. Additionally, CN is used as a pest control agent. In some plants, it is present in the form of cyanogenic glycosides, such as amygdalin in bitter almond and apricot cherry seeds.⁵ Cassava roots, yams, sorghum, maize are other cyanogenic plants which can cause toxicity if consumed without proper preparation.⁶ CN has a long history as a chemical weapon.⁷ Its low production cost, wide abundance and high toxicity makes CN a possible terror threat.⁸ In ancient Egypt, CN containing plants were used to punish criminals sentenced to death.⁷ Greeks and Romans used CN containing bitter almond and cherry laurel leaves against criminals and enemies. Having a boiling point of 26°C for HCN and being lighter than air made it more suitable as a warfare agent. The Nazi regime used it for executions in extermination camps during the World War II.⁷

Inhalation of HCN causes rapid intoxication while the oral exposure to cyanide salts is followed by a slower absorption in the gastrointestinal tract. CN has a high affinity for

cobalt and iron in the body. The concentration of CN in the circulation determines the toxicity response. Higher concentrations of CN (higher than five times LD50) result in rapid hyperventilation, loss of consciousness, convulsion, and finally death from cardiac and/or respiratory arrest. HCN smells like almonds, gives a metallic taste in the mouth, and causes apprehension and dyspnea (difficulty in breathing).⁹

Current Cyanide Antidotes and their Drawbacks

The currently available CN antidotal therapies in the United State are Cyanokit® and Nithiodote™. Nithiodote™ is a combination of thiosulfate (TS) and nitrite (NT).¹⁰ The sulfur donor TS reacts with CN to form the less toxic thiocyanate (SCN). NT has dual effect against CN. In the blood, NT converts hemoglobin to methemoglobin, which has a higher affinity for CN and forms a relatively stable CN-methemoglobin complex. The formed complex can react with TS to produce SCN preventing CN from binding to the cytochrome c oxidase. In addition, some of the NT will be converted into nitric oxide (NO) due to a series of biological reactions.¹¹ NO can alter the binding of CN to cytochrome c oxidase. This is done by displacing the CN from reaching the binding cite.^{12,13} Due to this dual effect, NT acts as an efficient CN antidote. Hydroxocobalamin, the active component of Cyanokit®, contains a cobalt (I) ion that is capable of forming a coordinative bond with CN.¹⁴

Both of the above drugs have limitations making them less useful in mass scenarios of CN intoxication. A common drawback of both antidotes is that they require intravenous (IV) administration needing trained personnel to treat multiple victims.¹⁵ Additionally, Cyanokit® requires high volumes of injection.¹⁶

The reaction between TS and CN is highly dependent on the mitochondrial sulfurtransferase enzyme, rhodanese (Rh). Since TS is an ionic compound, it cannot easily penetrate through the mitochondrial membrane to reach the endogenous Rh.¹⁷ Injecting free Rh directly to the circulation has other limitations, since the free enzyme can be destroyed by macrophages. Carriers such as erythrocytes and polymers have been tested in the past to encapsulate Rh prior to the IV administration.^{18,19} Excess amounts of NT can lead to methemoglobinemia preventing the natural oxygen transportation by the hemoglobin molecules.²⁰

Dimethyl Trisulfide (DMTS)

DMTS⁸ is a natural garlic compound that is used as a food additive. Allicin, the major garlic component, which gives the characteristic garlic odor, can be extracted with water or ethanol. Allicin can undergo different reactions to produce various di- and polysulfide compounds.²¹ Sulfur containing compounds in garlic, such as DMTS and diallyl disulfide, have been investigated as a CN antidote.²² DMTS is also found in many natural sources such as aging beer, cabbage, broccoli, cauliflower and fungating cancer wounds.^{23,24,25,26}

At Sam Houston State University, application of DMTS as a CN antidote and its formulation as a CN antidote have been patented by the Petrikovics lab under the title of CN antidote compositions (US 20150290143 A1, 2015; US 20150297535 A1, 2015).^{27,28} Unlike TS, DMTS can convert CN to SCN with high efficiency even without Rh, and has higher antidotal potential than TS. The IM administration makes DMTS superior over the Nithiodote™ and the Cyanokit™ as victims can self-administer the antidote during CN exposures.⁸

Blood Brain Barrier (BBB)

Brain is one of the essential organs of the body. Sensitive neurons in the brain require protection from xenobiotics. The BBB is a highly selective structural and biochemical barrier in the blood vessels of the brain. The constituents of BBB are the capillary endothelial cells, the basal lamina, astrocyte end-feet and tight junctions.^{29,30} Tight junctions among the endothelial cells in the BBB prohibit paracellular passing of molecules and promotes transcellular transport.³¹ Small molecules such as oxygen and ethanol can diffuse through the lipid membranes. Large hydrophilic molecules do not cross the BBB unless they are supported by transcytosis.²⁹ The major functions of the BBB are the following: controlling molecular traffic to supply essential nutrients, keeping toxic chemicals away and removing waste products, regulating the ion exchange, and maintaining ionic composition in brain fluid without fluctuations.²⁹ There are seven possible ways for a molecule to cross the BBB³²: cell migration, passive diffusion, carrier mediated efflux or influx, receptor mediated transcytosis, adsorptive mediated transcytosis, and tight junction modulations. Among these methods, passive diffusion is the most favored way for lipophilic small molecules such as DMTS to cross the BBB.

Parallel Artificial Membrane Permeability Assay (PAMPA)

Drugs should pass several biological membranes (skin, intestinal mucosa, BBB, etc.) to reach their receptors from the site of administration. Studying the penetration through these membranes leads to a better understanding of the absorption, distribution, metabolism and excretion of the drug. Different types of models exist for biological membranes, such as Caco-2, MDR1-MDCKII and PAMPA to model the drug permeability. Caco-2 is a model developed to measure the drug permeability through the

intestinal epithelial cells.³³ The preparation of this model requires about twenty days in a protected, sensitive environment.³⁴ MDR1-MDCKII is a model that mimics BBB penetration.³⁵ Recently, it was found that the *in-vitro* PAMPA model has higher correlation to the *in situ* brain perfusion assay than the other *in-vitro* MDR1-MDCKII model for a set of CNS drugs.³⁶

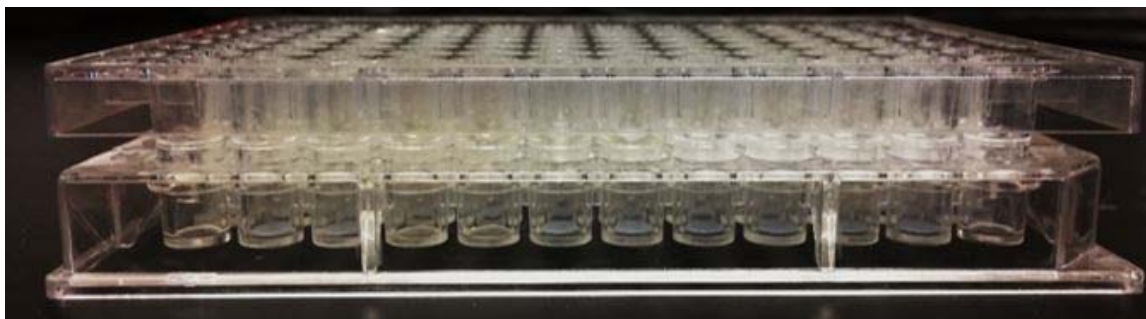


Figure 2. PAMPA Sandwiched Plates. The coupled acceptor and donor plates are called a PAMPA sandwich.

The PAMPA system contains two parallel plates which are paired together to make the “PAMPA sandwich” (Figure 2). The top plate (acceptor phase), shown in Figure 3, contains the solvent without the drug. The bottom of the acceptor compartment is an artificial membrane made of PVDF (polyvinylidene fluoride). This membrane is impregnated with a 2% porcine brain lipid extract.^{37,38} The lower plate (donor phase), shown in Figure 4, contains the test drug in a buffer solution maintained at pH 7.4. The sandwich is incubated for the desired time intervals to allow the drug crossing the membrane. The PAMPA model can be considered as a less expensive, more precise and more efficient BBB assay technique compared to the high-throughput screening methods, Caco-2 cells and the MDR1-MDCKII model.^{36,39} The PAMPA system is capable of modelling only passive diffusion through the BBB.

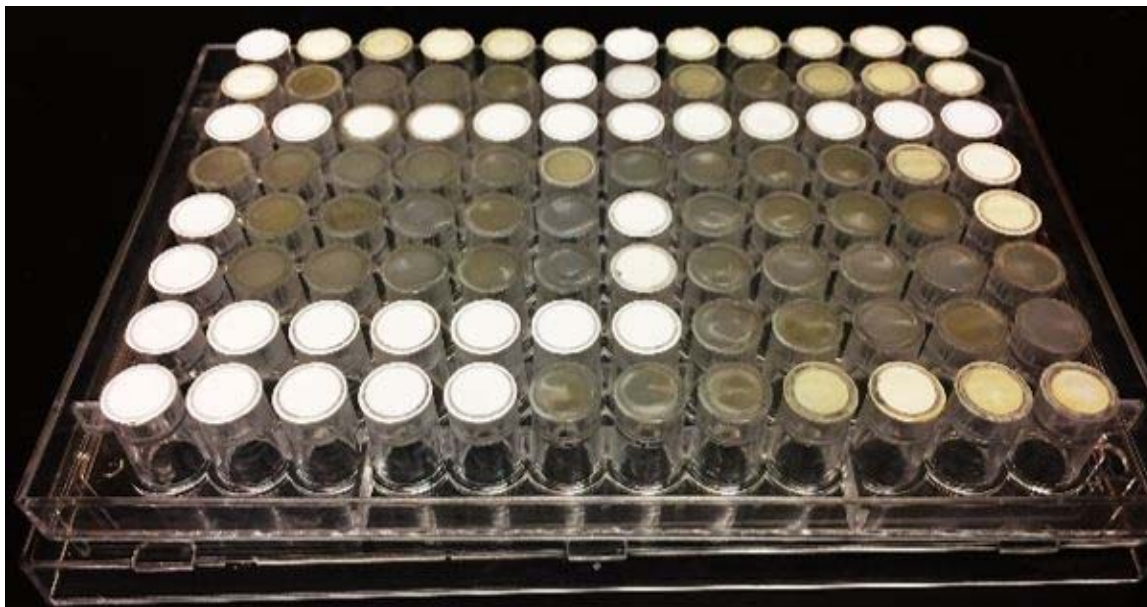


Figure 3. PAMPA Membranes on the Bottom of the Acceptor Plate. The membranes impregnated with 2% porcine brain lipid solution look transparent.

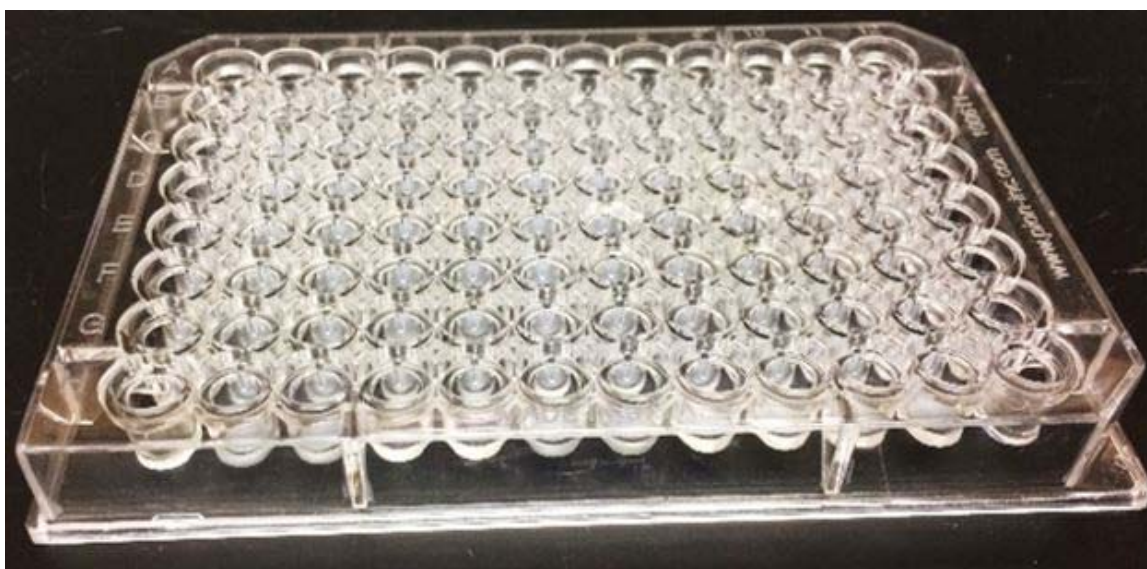


Figure 4. PAMPA Donor Plate. The donor plate is the holder for the acceptor phase in the PAMPA sandwich.

Particle Size Determination and the DLS Instrument

Dynamic Light Scattering (DLS) (Zetasizer Nano ZS, Malvern Instruments Ltd.) was used for particle size determination in the range of 0.3 nm to 10 μ m. Other than the size determination, the Zetasizer can be used to characterize the molecular weight and the

surface zeta potential of the test molecules. The instrument uses a 633 nm red laser as the light source.⁴⁰

Figure 5 shows a block diagram of the Zetasizer nano ZS. The intensity of light reaching the detector is controlled by the attenuator. Particles inside the cell scatter the light in all the directions. The detector is placed in a position where it can collect the scattered light coming from an angle of 173° . The scattered light does not have to travel through the whole sample cell due to the backscatter angle. This reduces the probability of the light scattering from more than one particles. The dust particles scatter the light to the forward direction, thus removing the scattered light from the dust particles is another advantage.⁴⁰

In the DLS technique the light is scattered over the sample and the fluctuations are measured over a period. The fluctuation of intensity of the scattered light is correlated to the size of the particles by a set of mathematical distributions.⁴¹ The DLS technique is widely used to characterize nanoparticles such as liposomes and micelles.^{42,43,44}

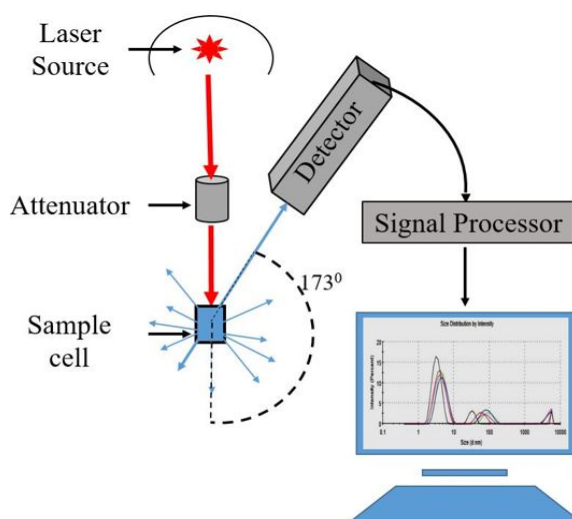


Figure 5. Block Diagram for the DLS Instrument, Zetasizer Nano ZS. The particle size distribution reported as a size correlogram in the connected computer.

CHAPTER II

MATERIALS AND METHODS

Chemicals

All the chemicals used were the form of their highest purity that are commercially available. DMTS and dimethyl disulfide (DMDS) were purchased from Sigma-Aldrich (Milwaukee, WI, USA), potassium cyanide from Sigma-Aldrich (Milwaukee, WI, USA), sodium thiosulfate from Alfa Aesar (Ward Hill, MA, USA) and sodium nitrite from Alfa Aesar (Ward Hill, MA, USA). Acetonitrile and water (for HPLC) were purchased from Acros Organics (Thermo Fisher Scientific, Geel, Belgium) and poly80 from Alfa Aesar (Ward Hill, MA, USA). For the *in-vivo* efficacy studies, male CD-1 mice (Charles River Laboratories, Inc., Wilmington, Massachusetts, USA) were kept in a light- and temperature-controlled room at 22 °C with a 12-hour light and dark full-spectrum constant lighting cycle. They were fed with water and 4% Rodent Chow (Harlan Laboratories Inc., Indianapolis, Indiana, USA) ad libitum. Animal procedures were conducted according to the guidelines in “The Guide for the Care of Laboratory Animals” (National Academic Press, 2011) in a facility accredited by the Association for Assessment of Laboratory Animal Care, International. Surviving animals were terminated at the end of the experiments according to the American Veterinary Medical Association Guidelines. Experiments were approved by the Institutional Animal Care and Use Committee (IACUC) at Sam Houston State University (IACUC Permission number: 15-09-14-1015-3-01).

Instruments

The following instruments were used for analysis (Table 1).

Table 1

Instruments Used for the Research.

Instrument	Brand and Model	Location
HPLC	Thermo Scientific Dionex Ultimate 3000	Dr. Petrikovics' Lab
Ion chromatograph	Thermo Scientific Dionex ICS 1500	Dr. Petrikovics' Lab
DLS instrument	Malvern Instruments Zetasizer nano ZS	Dr. Petrikovics' Lab
PAMPA system	pION BBB-PAMPA System	Dr. Petrikovics' Lab
Dropping ball viscometer	RCI Dropping Ball Viscometer	Dr. Williams' Lab

Methods

Preparation of DMTS Formulations DMTS-F1 and DMTS-F2.

Formulation 1 containing 50 mg/mL DMTS in 15% (w/w) poly80 was prepared according to the patented protocol by the Dr. Petrikovics' lab (US20150297535, 2015).^{28,45} Using an analytical scale 7.500 g poly80 was measured into a 50 mL VWR glass bottle followed by 42.500 g of HPLC grade water. The mixture was stirred for 30 minutes using a 3 cm stir bar. If the solution was clear after 30 minutes of stirring, the bottle was kept at 4°C for at least 6 hours prior to use. The solution was labelled "15% poly80" and used to dissolve DMTS weighed in to a volumetric flask to give final concentration of 50 mg/mL.



Figure 6. Preparation of the DMTS-F1. A solution of 15% poly80 was used as the media for DMTS.

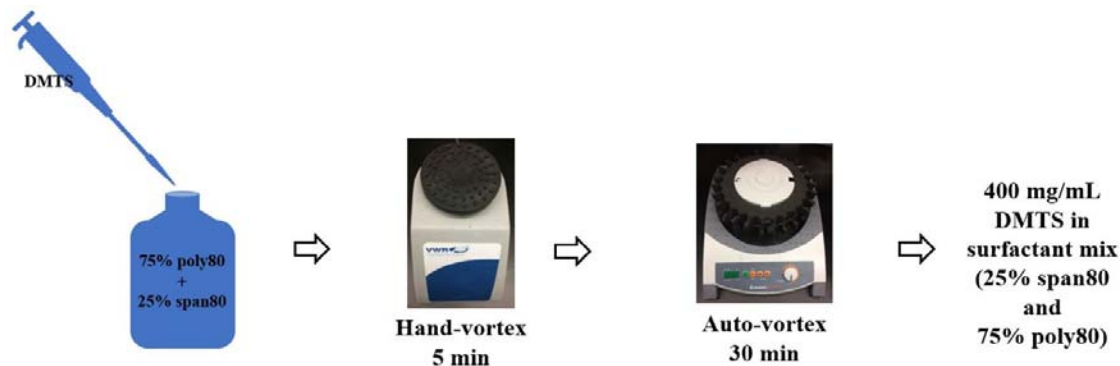


Figure 7. Preparation of DMTS-F2. A mixture of poly80 (75%) with span80 (25%) was used as the dispersant media for DMTS.

DMTS-F2 was prepared according to the protocol provided by the Southwest Research Institute (SwRI), San Antonio, Texas. This formulation contains poly80 and span80, but no water. An amount of 2.250 g of poly80 and 0.750 g span80 were weighed into a 10 mL glass vial, then DMTS (2.000 g) was added. The resulting mixture was hand-vortexed (VWR Fixed Speed Mini Vortex) for 5 minutes, followed by auto-vortexing (2000 rpm speed) (Heidolph Multi Relax Auto-vortex) for 5 minutes, which gave a clear solution. DMTS-F1 and DMTS-F2 preparations are illustrated in Figure 6 and Figure 7.

Analytical Method Development for CN by IC.

The purpose of this study was to establish in-house analytical methods using IC to determine CN, TS and NT in experimental solutions before use in the *in-vivo* and *in-vitro* studies. The stock solution of potassium cyanide (KCN) was prepared by Dr. Ilona Petrikovics and Dr. Lorand Kiss following the safety protocols in the lab (solution label: 20 mg/mL-KCN, IP/LK 10-30-2015). Seven calibration standards were prepared with CN concentrations of 0.000, 0.100, 0.200, 0.500, 1.00, 1.50, and 2.00 mg/mL from the stock solution. Samples were analyzed by the Thermo Scientific Dionex ICS 1500 Ion Chromatograph system. The flow rate was set to 1 mL/min. Dionex AS22 eluent concentrate (product number 063965) containing sodium carbonate and sodium bicarbonate (final concentration: 4.5 mM / 1.4 mM, respectively) was used as the mobile phase after dilution. Signals of the conductivity detector were recorded for the different CN concentrations in triplicates. The peak at 4.9 minutes was directly proportional to the CN concentration, therefore the area of this peak was plotted against the concentration for each CN standard solution.

Analytical Method Development for TS by IC.

A preliminary test was carried out to see the relationship of the peak area to the TS concentration. Three solutions of sodium thiosulfate with 0.005, 0.010 and 0.050 mg/ mL concentrations were prepared. Samples were analyzed by the Ion Chromatograph system (Thermo Scientific Dionex ICS 1500). The flow rate of the system was set to 1 mL/min. Dionex AS22 eluent concentrate (product number 063965) containing sodium carbonate and sodium bicarbonate (final concentration: 4.5 mM and 1.4 mM, respectively) was used as the mobile phase after dilution. The signals of the conductivity detector were recorded

for the different concentrations in triplicates. The peak at 17.5 minutes was directly proportional to the concentration, therefore the area of it was plotted against the concentration of TS.

Analytical Method Development for NT by IC.

A stock solution of NT with 16 mg/mL concentration was prepared. A series of solutions with NT concentrations of 0.000, 0.006, 0.012, 0.025, 0.050, 0.100, 0.200, 0.400, and 0.800 mg/ mL were prepared from the stock solution. Samples were analyzed by the Ion Chromatograph system (Thermo Scientific Dionex ICS 1500). The flow rate of the system was set for 1 mL/min. Dionex AS22 eluent concentrate (product number 063965) containing sodium carbonate and sodium bicarbonate (final concentration: 4.5 mM / 1.4 mM, respectively) was used as the mobile phase after dilution. The signals of the conductivity detector were recorded for the different concentrations in triplicates. The peak at 4.1 minutes was directly proportional to the concentration, therefore the area of it was plotted against the concentration of NT standard to get the calibration curve.

Analytical Method Development to Determine DMTS in the PAMPA system by HPLC-UV.

A method to analyze DMTS in blood by HPLC-UV has been published earlier by Dr. Petrikovics' lab.⁴⁶ This method was modified to meet the low DMTS concentration levels and non-blood medium of the PAMPA samples.

Calibration Curve 1 and the PAMPA Analysis of DMTS-F1.

The sample preparation was initiated by pipetting 40 μ L liquid out of the acceptor or the donor well or the calibration standard solution to a HPLC vial containing a glass insert with polymer feet (part number: 5181-1270, Agilent technologies). Then an aliquot

of 60 μL of 0.05 mg/mL DMDS in acetonitrile was added to the glass insert. The glass insert holds the sample higher inside the vial for a successful injection. DMDS was used as the internal standard to avoid injection errors. The vial was closed tightly with a screw-type cap, auto-vortexed for 10 seconds and mounted in an autosampler of the Dionex Ultimate 3000 (Thermo Scientific, Waltham, MA, USA) HPLC-UV instrument in Dr. Petrikovics lab. From the 100 μL sample mixture 40 μL was injected to the guard column (Product number: KJ0-4282, Phenomenex) connected to the 250 x 4.60 mm non-polar C-8 analytical column (Product number: 00G-4250-EO, Phenomenex Luna, pore size of 100 Å, outer diameter 5 μm). The mobile phase consisting of 35% water and 65% acetonitrile was used with a 1 mL/min flow rate with isocratic mode. The absorbance of the eluate was monitored at 215 nm by a UV detector. Formulation 1 (50 mg/mL DMTS) was diluted with 15% poly80 to obtain a working solution of 10.0 mg/mL DMTS. Using serial dilution with BBB Prisma HT buffer (Pion Inc. P/N - 110151) the standard solutions of 0.025, 0.050, 0.100, 0.200, 1.00, 2.50 mg/mL were prepared and 40 μL from these solutions were added to glass vial inserts. To this solution an aliquot of 60 μL of 0.05 mg/mL DMDS in acetonitrile was added to make the standard curve. After the sequence run was completed, the chromatographic peaks were analyzed by the HPLC instrument software (Thermo Scientific Dionex Chromeleon 7 version 7.2.0.3765). The peak area ratios of DMTS and DMDS was plotted against the DMTS concentration to obtain the calibration curve 1. Using this calibration curve the low concentrations of DMTS in the PAMPA wells could not be quantized. Therefore, changes were made to increase the peak areas for DMTS. The concentration of the internal standard was increased by two-fold (from 0.050 mg/mL to 0.100 mg/mL) and the volumes were reduced by half (from 60 μL to 30 μL). Additionally,

the volume of the samples added to the vials were increased from 40 μL to 70 μL . This increased the ratio of the sample and the internal standard volume from 2:3 to 7:3. The injection volumes to the column were also increased from 40 μL to 60 μL .

Preparing Calibration Curve 2 and the Comparison of the Two DMTS formulations.

The sample preparation was initiated by pipetting 70 μL liquid out of the acceptor or the donor well or the calibration standard solution to a HPLC vial that has a glass insert with polymer feet (part number: 5181-1270). Then, an aliquot of 30 μL DMDS in acetonitrile (0.10 mg/ mL) was added to the vial insert. The vial was closed tightly with a screw type cap, auto-vortexed for 10 seconds and mounted in an auto-sampler. An aliquot of 60 μL from the vial was injected to the HPLC column. The mobile phase – a mixture of 35% water and 65% acetonitrile – was eluted with a 1 mL/min flow rate with an isocratic mode. The absorbance of the elution was monitored at 215 nm wavelength by a UV detector. DMTS-F1 (with 50 mg/mL DMTS concentration) was diluted with 15% poly80 to obtain a working solution of 1.0 mg/ mL DMTS. Using serial dilution with BBB Prisma HT buffer (Pion Inc. P/N - 110151) the standard solutions of 0.006, 0.012, 0.025, 0.050, 0.100, 0.200, and 0.400 mg/ mL were prepared and 70 μL from these solutions were added to glass vial inserts. To this solution an aliquot of 30 μL of 0.10 mg/ mL DMDS in acetonitrile was added to make the standard curve. After the sequence run was completed, the chromatographic peaks were analyzed by the HPLC instrument software (Thermo Scientific Dionex Chromeleon 7 version 7.2.0.3765). The peak area ratios of DMTS and DMDS was plotted against the DMTS concentration to obtain the calibration curve 1.

Determination of the BBB Penetration of DMTS in F1 and F2 Using the PAMPA System.

The PAMPA system 96 well microplates with pre-loaded stirrers were purchased (Product No: 120551, pION, Billerica, MA, USA). The donor compartments of the PAMPA plates were filled with the diluted Prisma HT buffer. It was prepared by the dilution of 6.25 mL of Prisma HT concentrate (Product No: 110151, pION) to 250 mL with HPLC purity water (Product number: 26830-0040, Acros Organics, Fair Lawn, NJ). The pH was adjusted to 7.4 with 1 M NaOH (Sigma-Aldrich, St. Louis, MO) solution using a digital pH meter (Orion Star A111 pH meter, Thermo Scientific). The two DMTS formulations, F1 and F2, were diluted with a Prisma HT buffer working solution to obtain the diluted DMTS solutions (F1/DS and F2/DS) with 1.00 mg/mL DMTS concentration, respectively. These solutions (200 μ L) were placed in the donor wells. First, 3-3 of the donor wells were filled with F1/DS and with F2/DS. The polyvinylidene difluoride (PVDF) membranes in the wells of the acceptor plate were then impregnated with 5 μ L of the 2% porcine brain lipids solution (Product No: 110672, pION). The acceptor wells were filled with 180 μ L of the Brain Sink Buffer (BSB, Product No: 110674, pION) containing 0.5 mg/mL poly80. The acceptor plate was mounted on the top of the donor phase and placed in the PAMPA stirrer box (Gut-Box, pION). The thickness of the Aqueous Boundary Layer depends on the stirring speed on the donor phase. The stirring speed was chosen to maintain the 40 μ m thick layer. The plates were incubated in the stirrer box (Gut-Box) for 10 minutes. Samples were drawn from both the acceptor and the donor wells and analyzed in HPLC to determine the DMTS concentrations. The same method was repeated for the 20, 30, 40, and 60 min samples.

Determining the Poly80 Effect on the DMTS Permeability in the PAMPA System.

The purpose of this experiment was to check if the presence of 0.5 mg/mL poly80 in the acceptor phase influences permeability. Three incubation times of 10, 30, and 60 minutes were used. The PAMPA setup was prepared as described in the previous method with two changes (Figure 8 and Figure 9).

1. In that description, all of the acceptor wells had 0.5 mg/ mL poly80, but here half of the acceptor phases were incubated only with BSB without poly80.
2. In previous method, there were two types of the donor phases (F1/DS and F2/DS), but in this analysis, all the donor phases contained only F1/DS solution and not F2/DS.

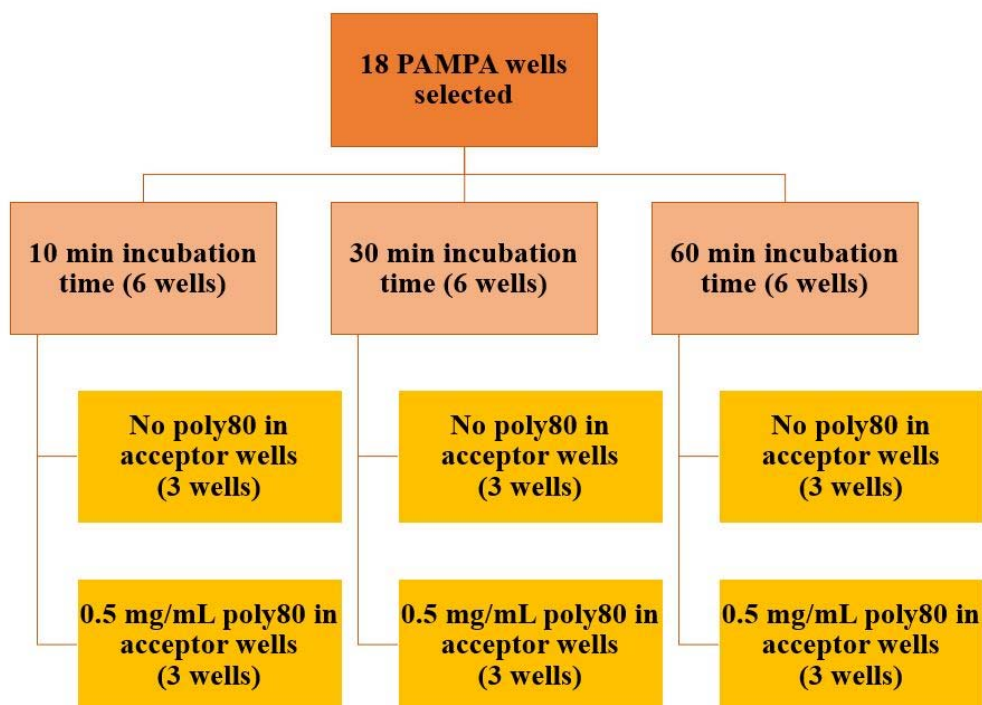


Figure 8. Experimental Setup to Determine the Effect of poly80 on DMTS Permeability. Samples were measured by HPLC-UV to determine the DMTS concentrations.

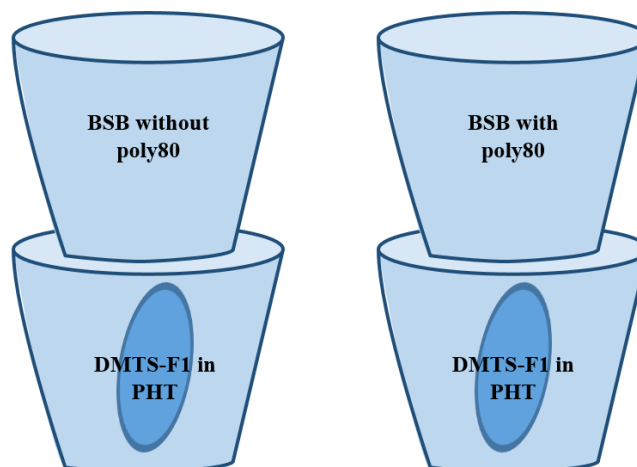


Figure 9. Effect of Poly80 in the Acceptor Wells on Permeability. The concentration of poly80 in the acceptor phase was maintained as 50 mg/mL.

Determining the Stirring Effect on the DMTS Permeability in the PAMPA System.

The purpose of this experiment was to check whether the presence of a stirrer in the acceptor phase has an effect on permeability. The PAMPA system was set up according to the method explained previously with several changes. The donor wells were filled only with the F1DS solution (1 mg/mL). Three time groups of the PAMPA wells were incubated (10, 30, and 60 minutes) and each time group had three subgroups. Subgroup 1: no stirrer in any of the wells (0 Sti), subgroup 2: one stirrer in the donor well and no stirrer in the acceptor well (1 Sti) and subgroup 3: one stirrer in the acceptor well and one stirrer in the donor well (2 Sti). Three parallels from each subgroup were analyzed (27 wells in total, Figure 10 and Figure 11). All the acceptor wells were filled with BSB without DMTS.

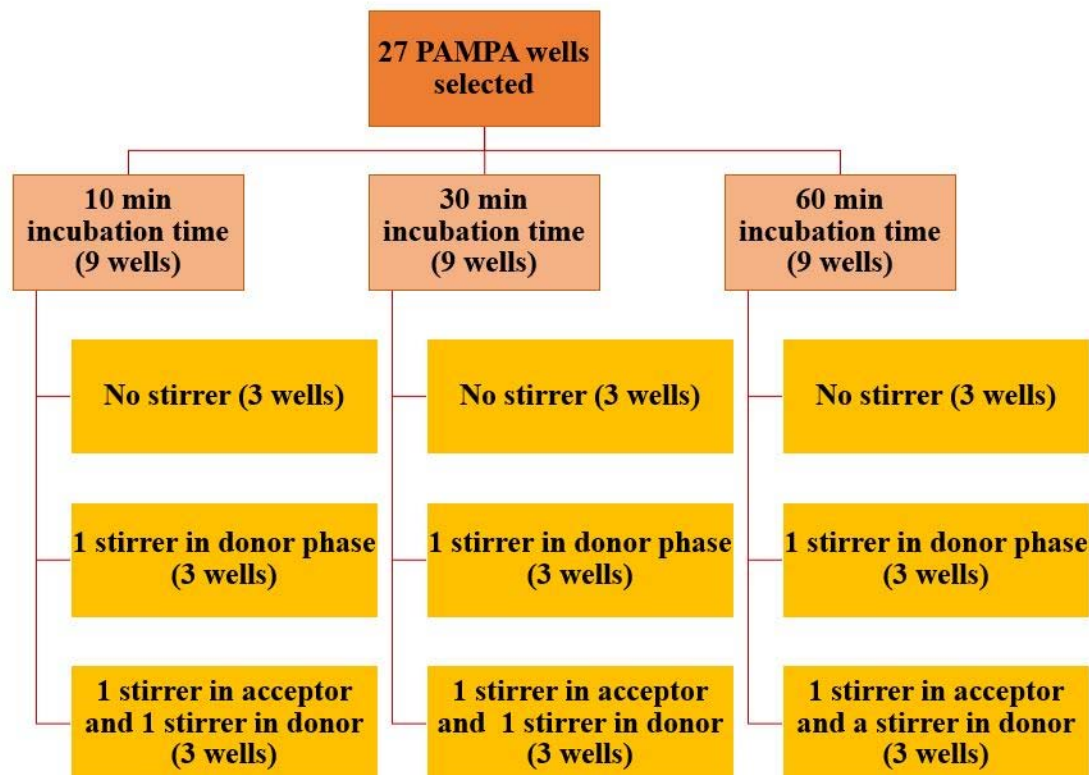


Figure 10. Effect of the Stirrers on DMTS Permeability. The sample were analyzed by HPLC-UV.

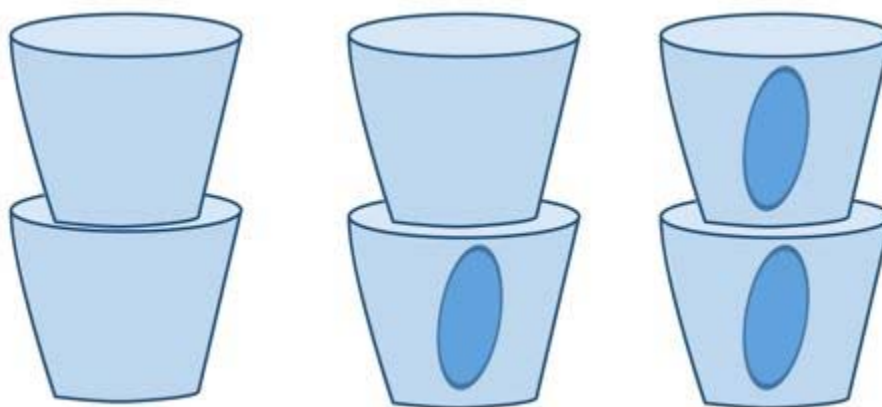


Figure 11. Placing Stirrers (0, 1, 2) in the Acceptor and the Donor Wells. The PAMPA system was stirred with a speed that resulted a 40 μm boundary layer.

Viscosity Determination of DMTS-F1 and DMTS-F2.

Purpose of this study was to determine the viscosities of two media of DMTS-F1 and DMTS-F2. It was required for the size distribution studies. The dropping ball viscometer (RCI, Model number: Y430) in Dr. Williams' lab was used for the analysis (Figure 12). The following equation was used for the calculations.

$$\eta = k (\rho_0 - \rho) t$$

Where η is the viscosity of the liquid, k is the viscometer constant, ρ is the density of the liquid, ρ_0 is the density of the metal ball and t is the time taken for the metal ball to pass through liquid passage. The density of the metal ball is 8.02 g/mL which was provided by the manufacturer. The value for ρ was determined by weighing the mass of 10.00 mL of the liquid using an analytical balance (Mettler Toledo, Product number: ML204/03). The values were transferred to the following equation:

$$\rho = \frac{\text{mass of the liquid aliquot}}{\text{volume of the liquid aliquot}}$$

The value for k is depending on the temperature according to the following equation of $k = -0.0088T + 0.0575$ (developed by Dr. Williams' lab), where T is the temperature of the liquid. The temperature was measured with a thermo-couple probe (Extech Instruments 383274 Multimeter) and found to be 25 °C. The viscometer was filled with the DMTS-F1 media solution (without DMTS). Care was taken to ensure that there were no air bubbles inside. The metal ball was inserted into the tube and the lid was closed after allowing excess liquid overflow. If any air bubbles were present in the tube, the liquid was refilled. The viscometer was then fixed to a movable clamp and turned upside down (180° reverse) in order to get the metal ball to the starting position. A digital video camera was focused on the liquid passage where the metal ball travelled. When everything was ready, the

viscometer was turned into the first position (180° forward) and allowing the travelling of the ball through the liquid passage. This was repeated three times and the video was analyzed to determine the t values. The whole process was repeated with the media of DMTS-F2 (mixture of poly80 and span80).

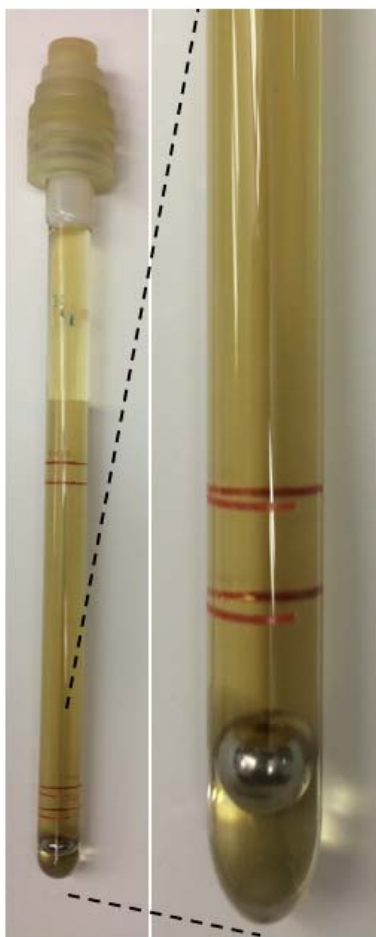


Figure 12. Dropping Ball Viscometer with the Travelling Metal Ball. The distance between the red lines represents the passage length which was used to calculate the value of t .

Droplet Size Distribution Determination.

These experiments were carried out to determine the time dependence of the droplet size distribution of the two formulations, DMTS-F1 and DMTS-F2 as a part of the storage stability characterization. A Zetasizer nano ZS (Malvern Instruments Ltd. UK) based on

DLS was used for the droplet size determination. For a more accurate droplet size determination, the knowledge of viscosity values is required. The disposable sample cell (Malvern, Product number: DTS0012) was filled with 1.5 mL of F1 and the cuvette was placed in the sample holder. The temperature of 25 °C, equilibration time of 120 seconds, measurement angle of 173° backscattering was selected as instrumental parameters for the droplet size measurement. The number of measurements were three, the time delay was 5 seconds between the samples, the viscosity of the media for F1 was 2.32 cP and for F2 511.00 cP. DLS analysis of DMTS-F2 produce no significant peaks which is likely due to its high viscosity.

Analytical Method Development to Determine DMTS concentrations in Blood by HPLC-UV.

The calibration curve was prepared to determine the DMTS concentration in blood samples collected from the pharmacokinetic studies. The method was divided into three sections: a) the preparation of the DMTS standard solutions, b) spiking the standards with blood and extraction, c) HPLC analysis of the samples to determine the DMTS concentrations.

- a) Preparation of the DMTS standard solutions. An 15% aqueous poly80 solution was prepared according to the standard preparation procedure to make a 10 mg/mL DMTS standard solution. By diluting the stock solution with 15% poly80 a series of working solutions with DMTS concentrations of 0.000, 0.010, 0.020, 0.040, 0.080, 0.160, 0.200, and 0.500 mg/mL were prepared. An internal standard solution of 0.1 mg/mL DMDS in acetonitrile was prepared.

- b) Spiking the standards with blood and extraction of the samples for HPLC injection. Into a 1.5 mL plastic vial (Eppendorf), 80 μ L of sheep blood and 10 μ L of heparin (10U/ mL) and 10 μ L from the relevant DMTS standard were added. The vial was hand-vortexed for five seconds. Three parallels were prepared from each standard. The final DMTS concentrations in the standard solutions after spiking were 0, 1, 2, 4, 8, 20 and 50 μ g/mL. To the spiked blood sample 200 μ L of the 0.1 mg/ mL DMDS internal standard solution was immediately added. Samples were then hand-vortexed for two minutes and auto-vortexed for 10 minutes (2000 rpm speed). The vials were centrifuged at 4°C at the speed of 14,000 rcf for 5 minutes. An aliquot of 150 μ L from the clear supernatant was pipetted to a HPLC vial that had a glass insert. Vials were closed tight and loaded on the auto-sampling tray of the HPLC.
- c) An amount of 100 μ L from the vial was injected to the guard column (product number: KJ0-4282) connected to the 250 x 4.60 mm non-polar C-8 analytical column having a Phenomenex Luna stationary phase consisting of bonded octane units coated on silica support particles (Product number: 00G-4250-EO, Phenomenex Luna, pore size of 100 Å, outer diameter 5 μ m). The mobile phase, a mixture of 35% water and 65% acetonitrile was used at a 1 mL/min flow rate in isocratic mode. Absorbance of the elution was monitored at 215 nm.

The ratio of the DMTS and DMDS peak areas were plotted against the DMTS concentrations to obtain the calibration curve.

Pharmacokinetics of the DMTS-F1 and DMTS-F2.

The purpose of the analysis was to determine the absorption kinetics of DMTS formulations F1 and F2. The amount of DMTS that reached the blood and the brain was determined at different time intervals following IM injection. For each formulation, a dose of 150 mg/kg was provided to male CD rats (Charles River Kingston, Stone Ridge, NY,) weighing 200-250 g. To reach the required dose the injection volume was calculated by the following equation:

$$\text{Volume of the injection } (\mu\text{L}) = \frac{\text{Mass of the rat (g)} \times 150 \left(\frac{\text{mg}}{\text{kg}}\right) \times \left(\frac{10^{-3} \text{kg}}{\text{g}}\right) \times \left(\frac{10^3 \mu\text{L}}{\text{mL}}\right)}{\text{DMTS concentration in the formulation } \left(\frac{\text{mg}}{\text{mL}}\right)}$$

DMTS concentrations for F1 and F2 were 50 mg/mL and 420 mg/mL respectively. If the calculated injection volume was higher than 150 μL , we used the two rear legs for injection. Blood was drawn (0.25 mL) using a 1 mL heparinized syringe at 0, 8, 16, 23, 30, 40, 60, and 150 minutes after the DMTS injection and was immediately transferred to a heparinized plastic vial (1.5 mL Eppendorf) (Figure 13). The heparin treatments of the vials were always prepared by adding constant volumes of heparin solution (10U/ mL) before adding the blood samples. Out of the total volume of 250 μL blood sample, a volume of 100 μL was pipetted to two heparinized microcentrifuge tubes. (This provided the duplicates for the rest of the analysis). The analytical method explained was used for determining DMTS concentration for the blood sample: To each microcentrifuge tube 200 μL of ice-cold acetonitrile containing 0.1 mg/mL DMDS was added immediately. Then the microcentrifuge tubes were hand-vortexed for 10 s and auto-vortexed for 10 minutes and centrifuged at 4 $^{\circ}\text{C}$ for 5 minutes at a speed of 14,000 rcf. A volume of 150 μL of the clear

supernatant from each vial was transferred to the glass inserts in the HPLC vials. The samples were analyzed with HPLC-UV with an injection volume of 100 μL .

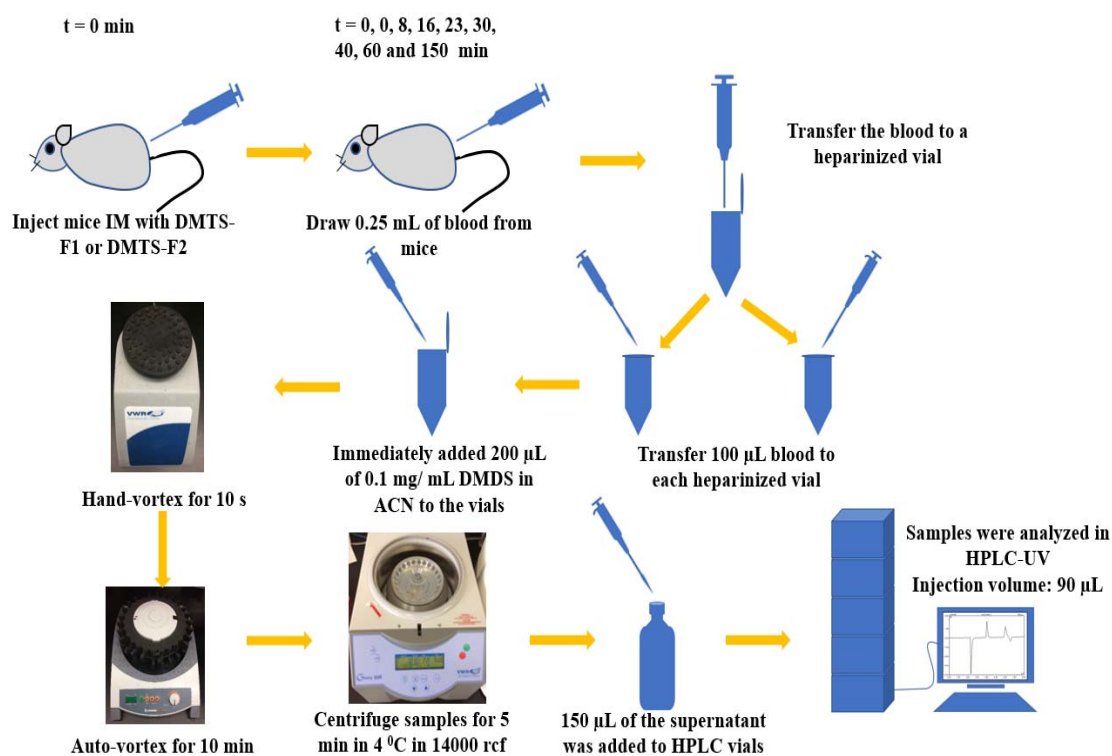


Figure 13. Flow Chart for the Pharmacokinetic Study. Mice were treated with F1-DMTS and F2-DMTS separately. The final extracted samples were analyzed for DMTS concentration by HPLC-UV.

CHAPTER III

RESULTS

Preparation of two DMTS Formulations based on Known Methods

Two formulations of DMTS, DMTS-F1 (50 mg/mL in 15% poly80) and DMTS-F2 (40% DMTS in the mixture of 25% span80 and 75% poly80) were prepared and stored for the experiments. The DMTS-F1 formulation was originally developed and published from Dr. Petrikovics' lab²⁸. The same formulation method was followed and the droplet sizes were measured using DLS instrument after the preparation of a DMTS-F1 solution. The majority of the droplets were within the range of 4 nm to 8 nm (above 50%), which confirmed the quality of the DMTS-F1 preparation (Table 2 and Figure 14).

Table 2

Particle Size Distribution of the DMTS-F1 Right After Preparation.

0 hours 25°C	Average Size (nm)	% Intensity
Peak 1	7	82
Peak 2	50	17
Peak 3	2796	1

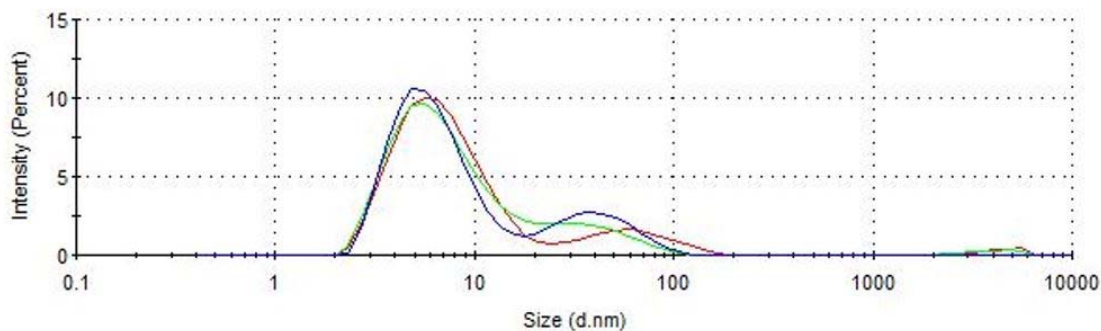


Figure 14. Droplet Size Distribution of DMTS-F1 Right After Preparation. The red, green and blue lines represent three measurements for the same sample. The major peak shows that the majority (78%) of the particles have a diameter of 7 nm.

DMTS-F2 was originally prepared in another research institute (SwRI). To verify the quality of the freshly prepared formulation, the F2 droplet size distribution was compared to that of the samples received from SwRI (Figure 15 to Figure 17). The higher level of overlapping of the size correlograms confirms the precision of the F2 formulation.

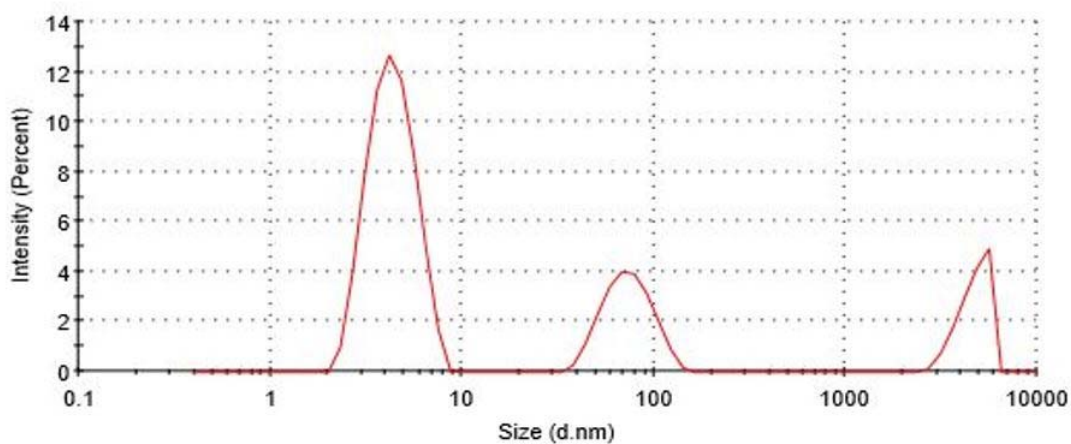


Figure 15. Droplet Size Distribution of the Original DMTS-F2 Received from SwRI. The correlogram shows three major peaks for the original formulation.

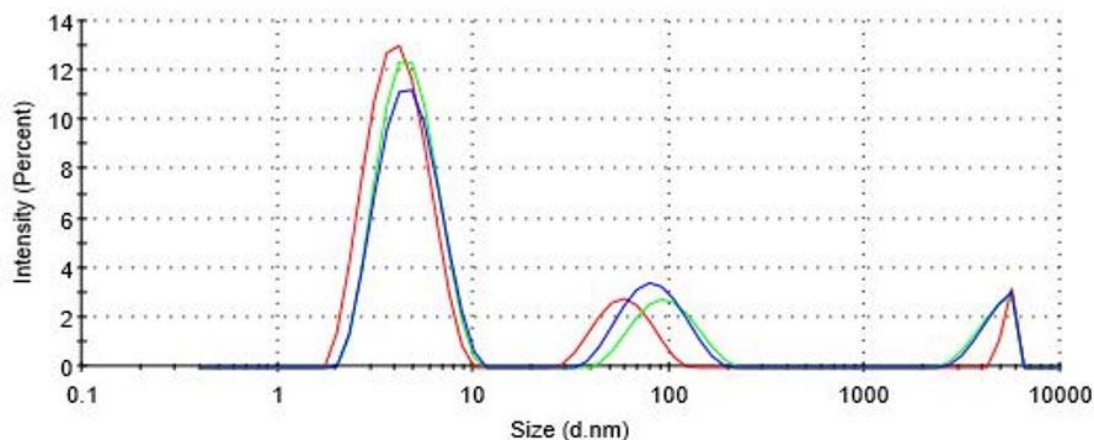


Figure 16. Droplet Size Distribution of the Freshly Prepared DMTS-F2. Red, blue and green colors for the three repeated DLS measurements of a single batch of the new formulation prepared in our lab.

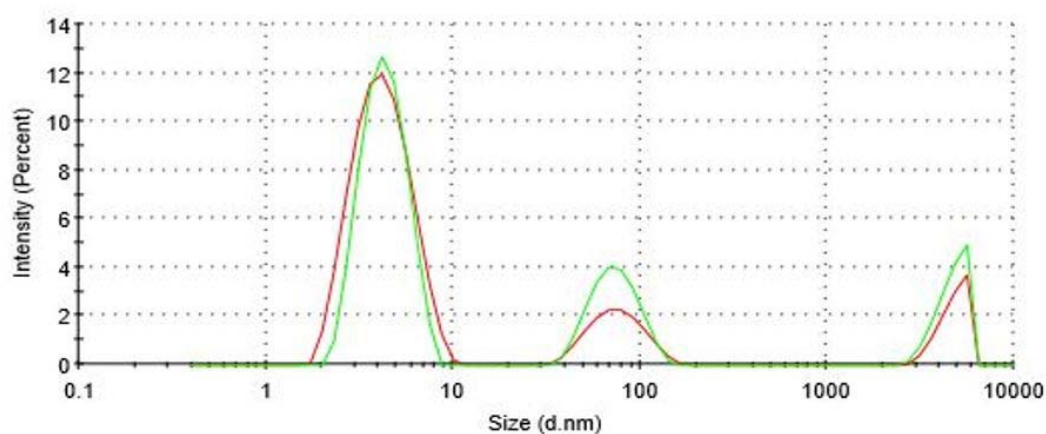


Figure 17. Comparison of the Droplet Size Distribution of the Freshly Prepared DMTS-F2 in Our Lab vs. the Original DMTS-F2 Sample Prepared by SwRI. The overlay of two correlograms shows that the two formulations have the same size distribution. The red line represents the fresh formulated DMTS-F2 and the green line represents the DMTS-F2 formulated earlier by SwRI.

Analytical Method Development for CN by Ion Chromatography (IC)

Five standard solutions with different concentrations of CN were prepared and analyzed by IC. The calibration curve for CN was set up as the CN concentrations were proportional to the peak areas in the chromatograms (Figure 18 and Figure 19).

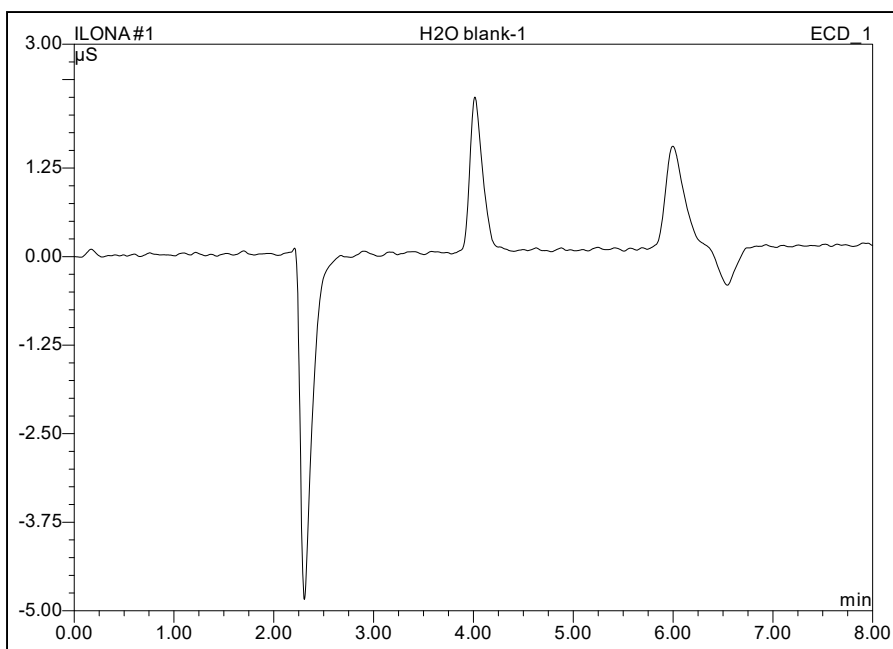


Figure 18. Ion Chromatogram for the CN Blank (0 mg/ mL CN). There was no peak at 4.9 min.

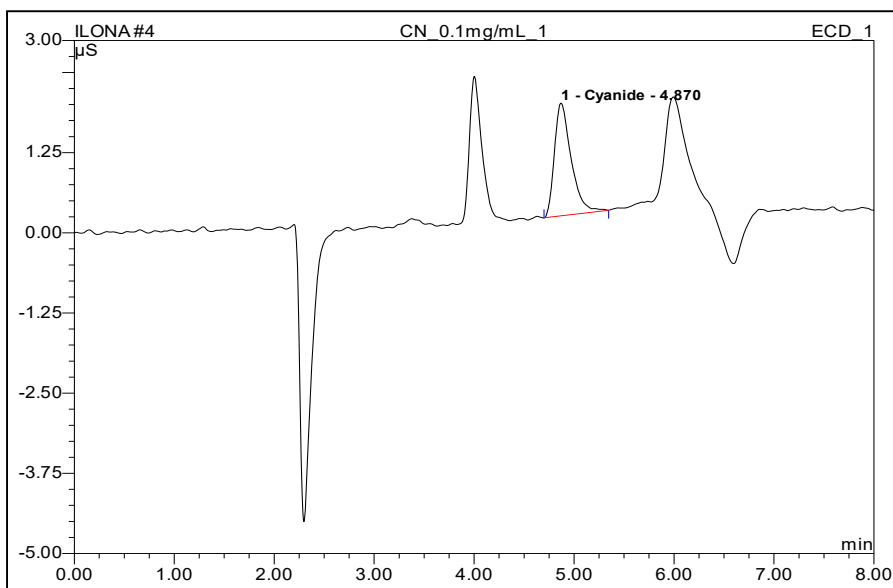


Figure 19. Ion Chromatogram for 0.1 mg/mL CN. The peak was observed at 4.9 mins. Increasing CN concentration resulted in increasing CN peak area.

Figure 20 represents the calibration curve made by plotting CN peak areas vs. CN concentrations. There was a good correlation between CN concentrations in the range of 0.1 mg/mL to 1 mg/mL with an R^2 value of 0.9968 and equation of $y = 2.85x + 0.06$. In

the calibration curve each data point represents the mean \pm SD ($n=3$). The calibration curve was prepared to measure and confirm the CN concentrations of the test solutions used in other *in-vivo* and *in-vitro* experiments such as efficacy studies and pharmacokinetics.

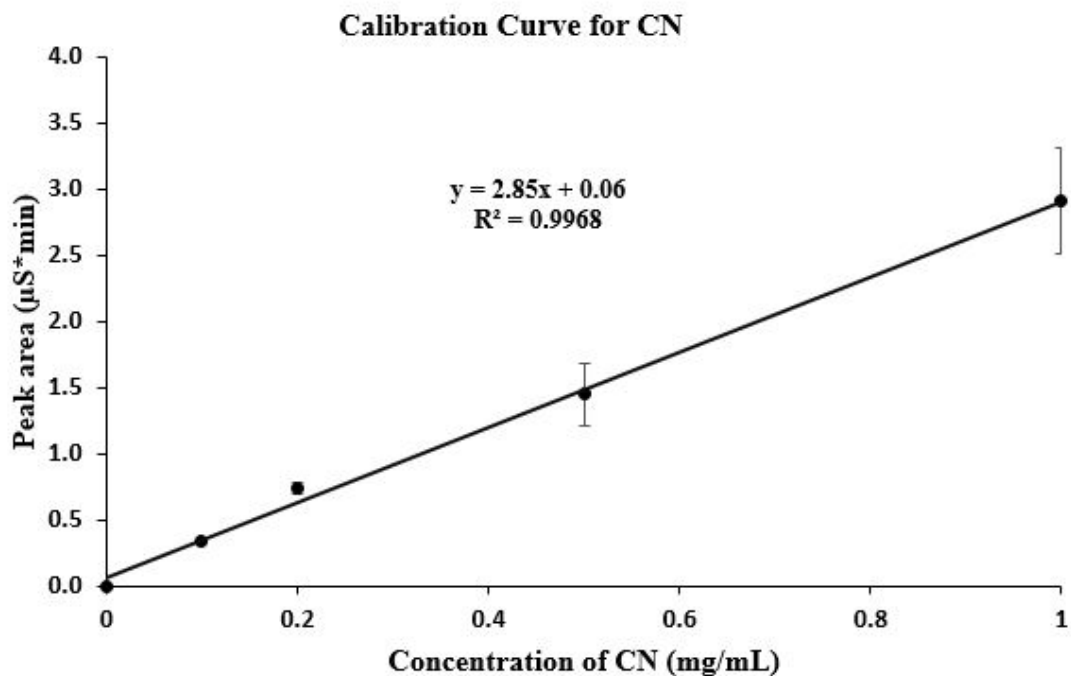


Figure 20. CN Calibration Curve Measured by IC. Data are presented as mean \pm standard deviation (S.D.); number of measurements (n) = 3

The limit of detection (LOD) and limit of quantification (LOQ) were determined for the calibration curve.⁴⁷

$$LOD = y_{blank} + 3s = 0.000 + (3 \times 0.008) = 0.024$$

$$Concentration\ LOD = 3s/m = (3 \times 0.225) / 2.85 = 0.008\ mg/mL = 8\ \mu g/mL$$

$$LOQ = y_{blank} + 10s = 0.000 + (10 \times 0.008) = 0.080$$

$$Concentration\ LOQ = 10s/m = (10 \times 0.008) / 2.8464 = 0.028\ mg/mL = 28.4\ \mu g/mL$$

Where y_{blank} is the mean of the blank signal, s is the standard deviation of the signal for the lowest analyzed concentration and m is the gradient of the calibration curve.

$$s = \sqrt{\frac{(x_m - x_i)^2}{n-1}}$$
 where x_m is the mean of the repeats, x_i is the individual value of measurement and n is the number of repeats for the lowest analyzed concentration.

Analytical Method Development for TS using IC

Four solutions with TS concentrations of 0.000, 0.005, 0.010 and 0.050 mg/mL were prepared and analyzed by IC. TS concentrations between 0.005 mg/mL to 0.05 mg/mL gave good correlation with the peak areas (Figure 21 to Figure 23). The resulting linear plot (Figure 24) had an R^2 value of 0.9997 and an equation of $y = 55.3x - 0.02$. These results were planned to be used for measuring TS for various applications such as *in-vitro* and *in-vivo* efficacy studies. Unfortunately, the IC instrument broke after the preliminary studies and further experiments will be carried out later once the instrument is repaired.

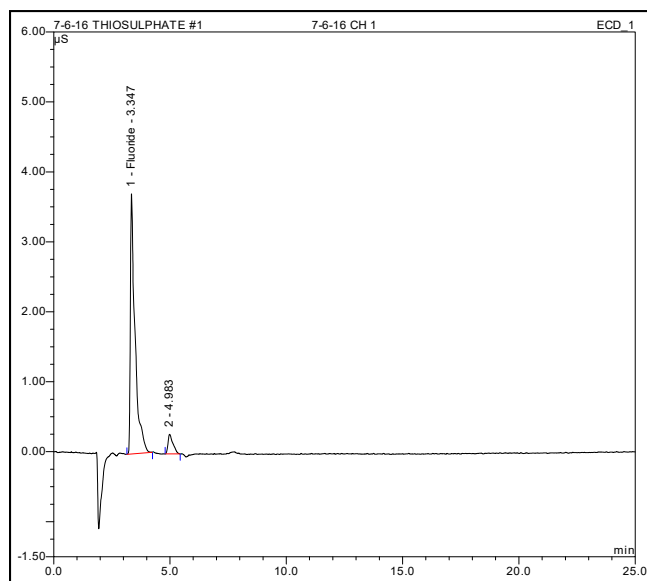


Figure 21. Ion Chromatogram for the TS Blank (0 mg/ mL). There was no peak at 17 min.

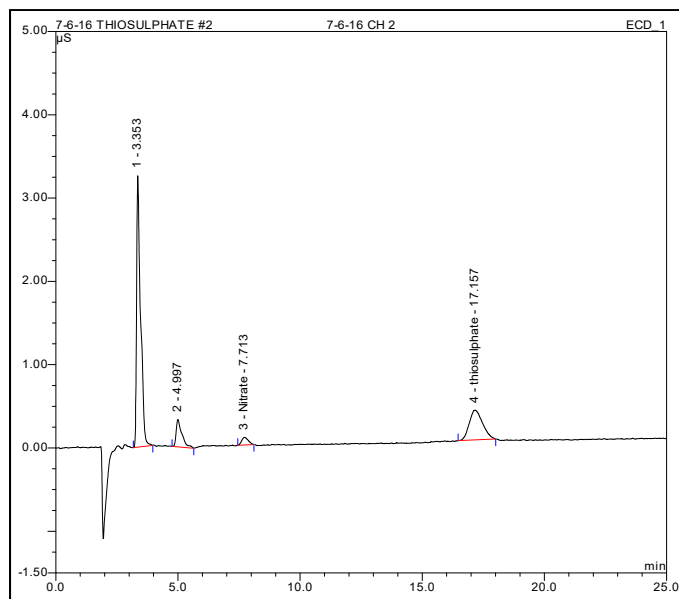


Figure 22. Ion Chromatogram for TS (0.005 mg/ mL). The TS peak was observed at 17 min.

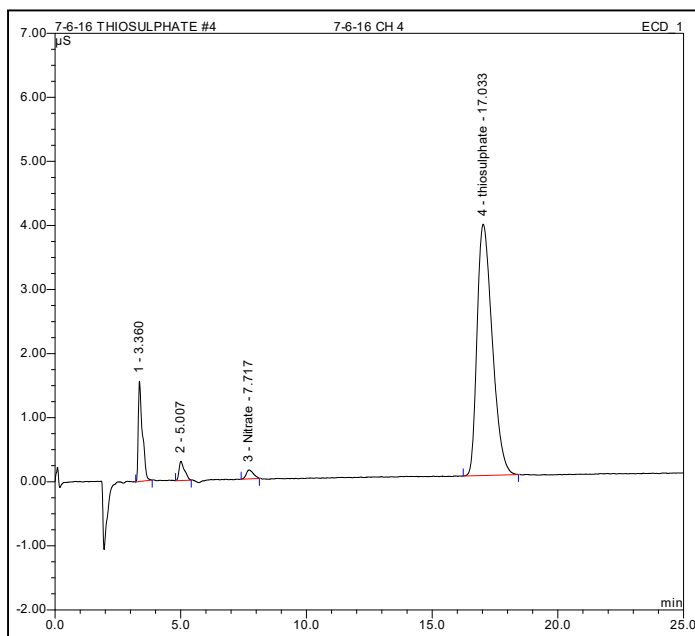


Figure 23. Ion Chromatogram for TS (0.05 mg/ mL). The peak was observed at 17 min. Increasing TS concentration resulted in increasing TS peak area.

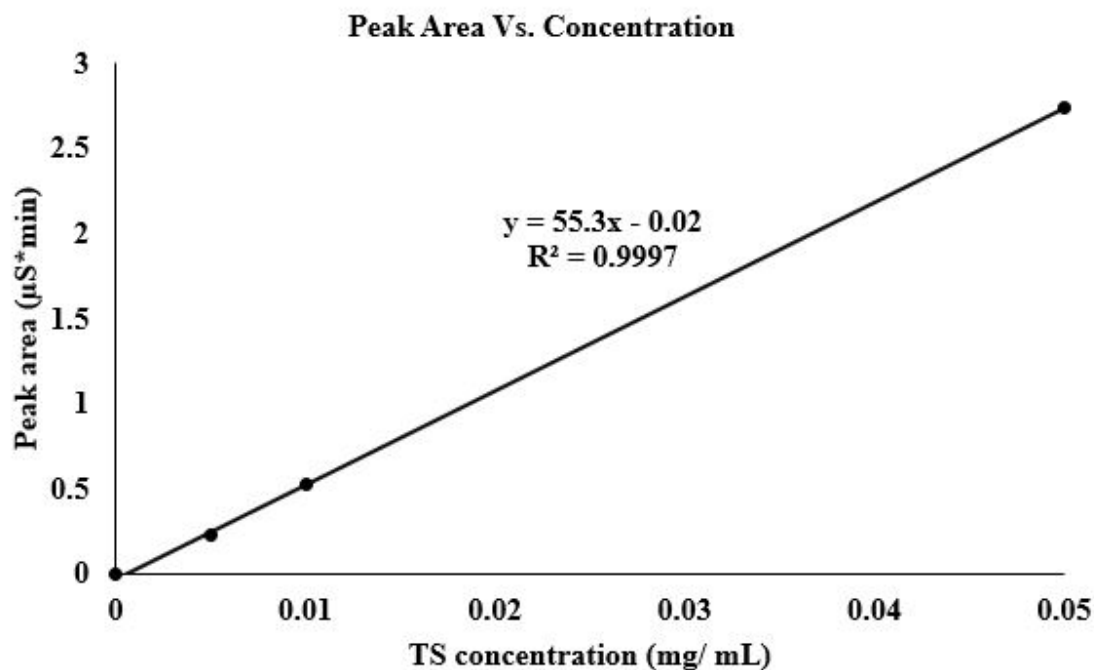


Figure 24. Peak Area vs. TS Concentration. The R^2 value indicates a good potential to develop an analytical method for TS using IC. As a preliminary experiment, each data point was measured only once.

Analytical Method Development for NT quantitation using IC

Nine solutions with NT concentrations of 0.000, 0.006, 0.012, 0.025, 0.050, 0.100, 0.200, 0.400, and 0.800 mg/ mL were prepared and analyzed by IC. NT concentration was proportional to the peak area of the peak appeared at 4 min (Figure 25 to Figure 27).

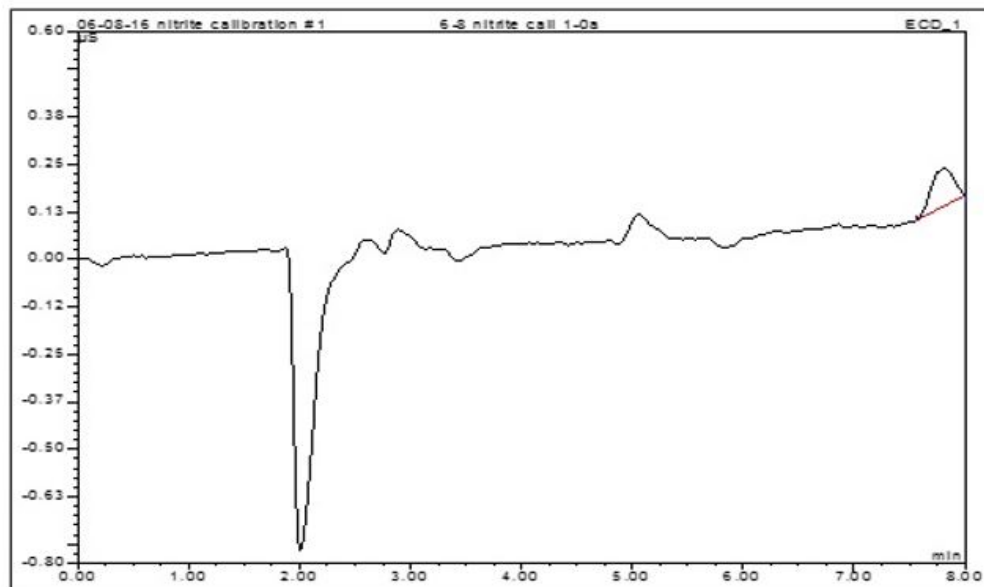


Figure 25. Ion Chromatogram for the NT Blank (0.000 mg/ mL NT). There was no peak at 4 min.

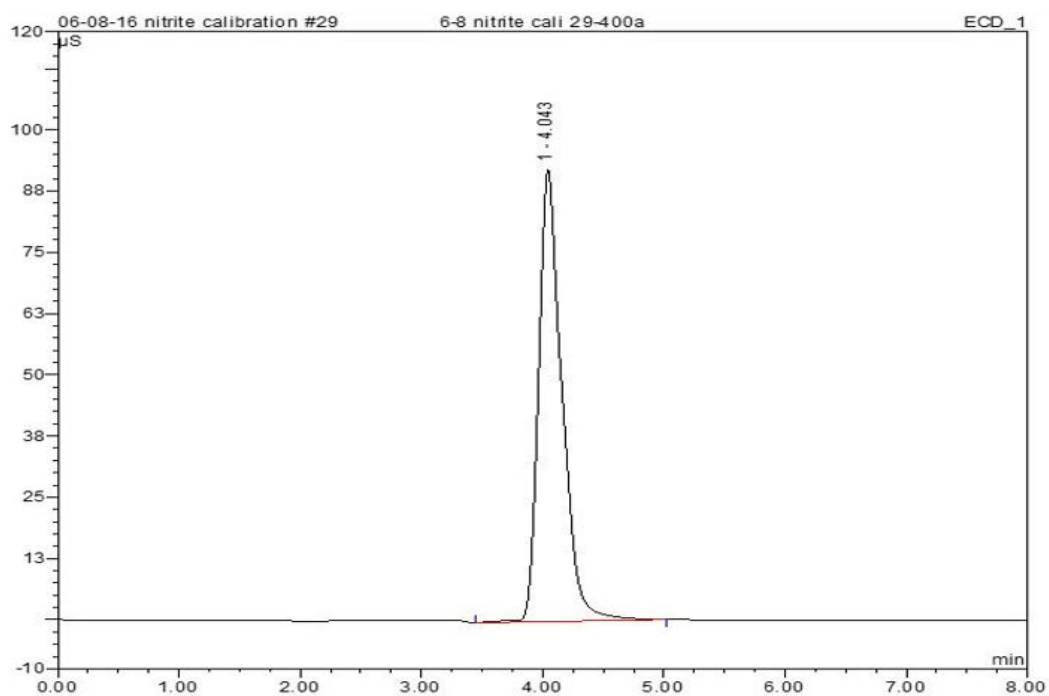


Figure 26. Ion Chromatogram for NT (0.100 mg/ mL). The peak was observed at 4 min.

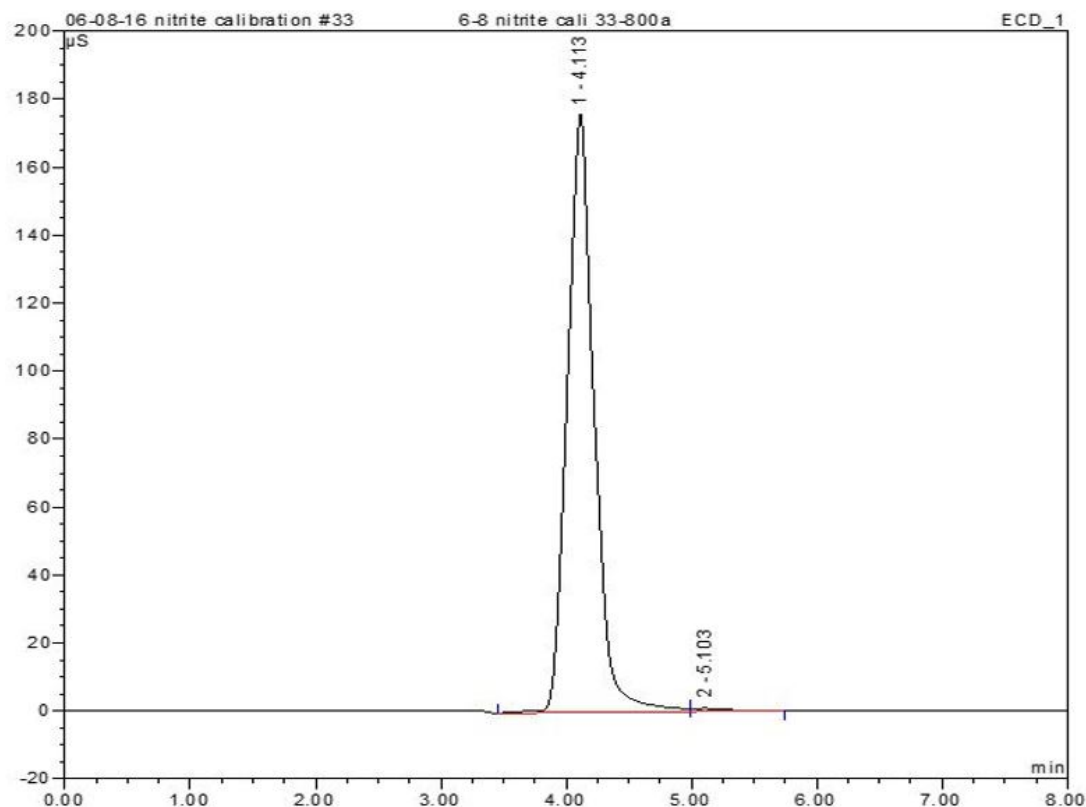


Figure 27. Ion Chromatogram for NT (0.800 mg/ mL). The peak was observed at 4 min. Increasing NT concentration resulted in increasing NT peak area.

NT concentrations between 6 μg/mL to 800 μg mL gave good correlation with the peak areas. The resulting linear plot, shown in Figure 28, had an R^2 value of 0.9987 and an equation of $y = 50.4x + 0.2$. The plan was to use these results to measure TS for various applications such as *in-vitro* and *in-vivo* efficacy studies.

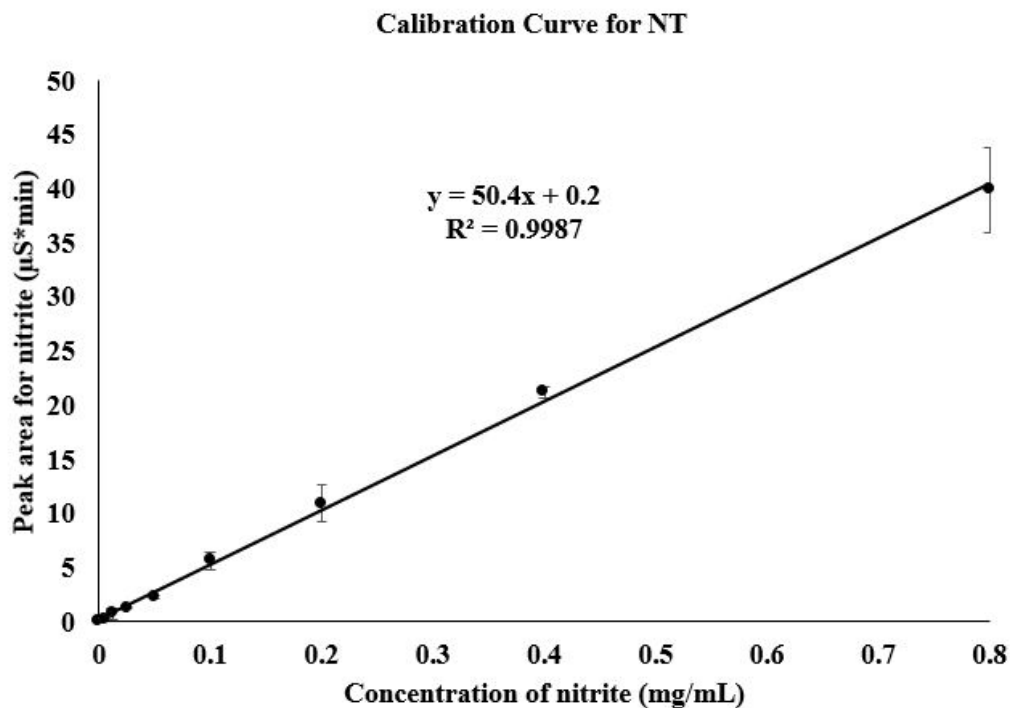


Figure 28. Calibration Curve for NT Using IC. Data are presented as mean \pm S.D., $n = 3$. Some error bars are not visible as the S.D. is low.

The limit of detection (LOD) and limit of quantification (LOQ) were determined for the calibration curve.

$$LOD = y_{blank} + 3s = 0.000 + (3 \times 0.092) = 0.276$$

$$Concentration\ LOD = 3s/m = (3 \times 0.092) / 50.4 = 0.005\ mg/mL$$

$$LOQ = y_{blank} + 10s = 0.000 + (10 \times 0.092) = 0.920$$

$$Concentration\ LOQ = 10s/m = (10 \times 0.0915) / 0.0504 = 0.018\ mg/mL$$

Where y_{blank} is the mean of the blank signal, s is the standard deviation of the signal for the lowest analyzed concentration and m is the gradient of the calibration curve.

$$s = \sqrt{\frac{(x_m - x_i)^2}{n-1}}$$

where x_m is the mean of the repeats, x_i is the individual value of

measurement and n is the number of repeats for the lowest analyzed concentration.

Analytical Method Development to Determine DMTS in the PAMPA System Using HPLC-UV

A calibration curve to determine the DMTS concentrations in PAMPA solutions was developed using the HPLC-UV detection. DMTS had a retention time of 8.2 min in the spectrum. DMDS was used as the internal standard for the analysis (Figure 29).

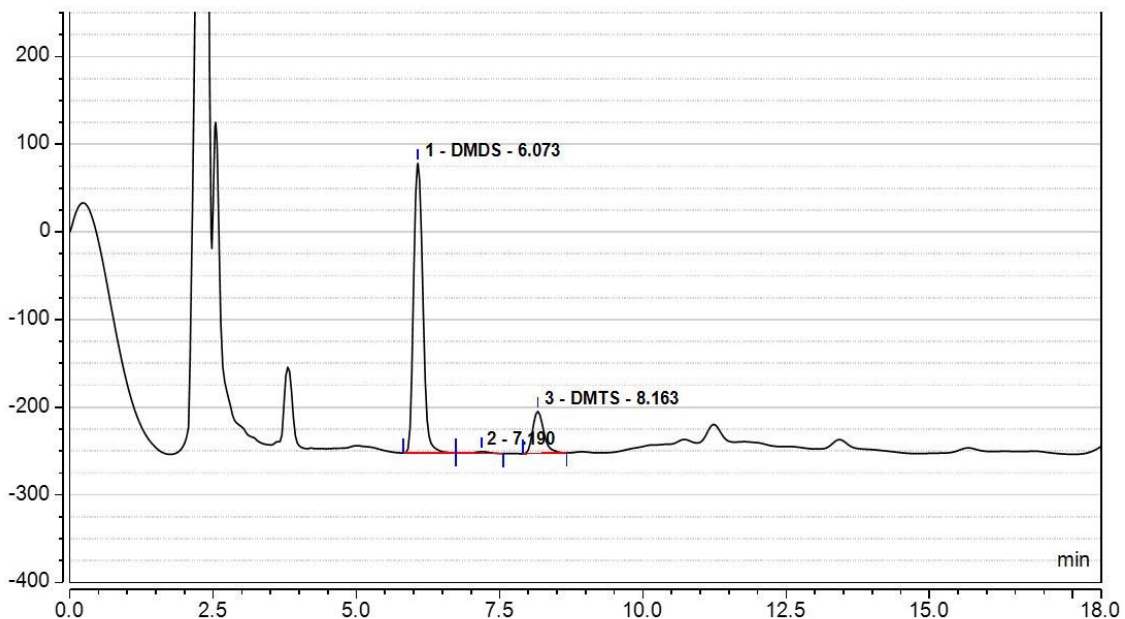


Figure 29. Characteristic HPLC-UV Spectrum Observed for DMTS. Retention times of the DMDS and DMTS peaks are 6.1 minutes and 8.2 minutes respectively.

The DMTS peak was clearly separated from other peaks. Peak areas of the two peaks, DMTS and DMDS, were determined and used for processing data.

Calibration curve 1 and the PAMPA analysis of DMTS-F1

After the sequence run was completed, the results were analyzed by HPLC software. Peak area ratios of DMTS/DMDS were plotted against DMTS concentrations (Figure 30).

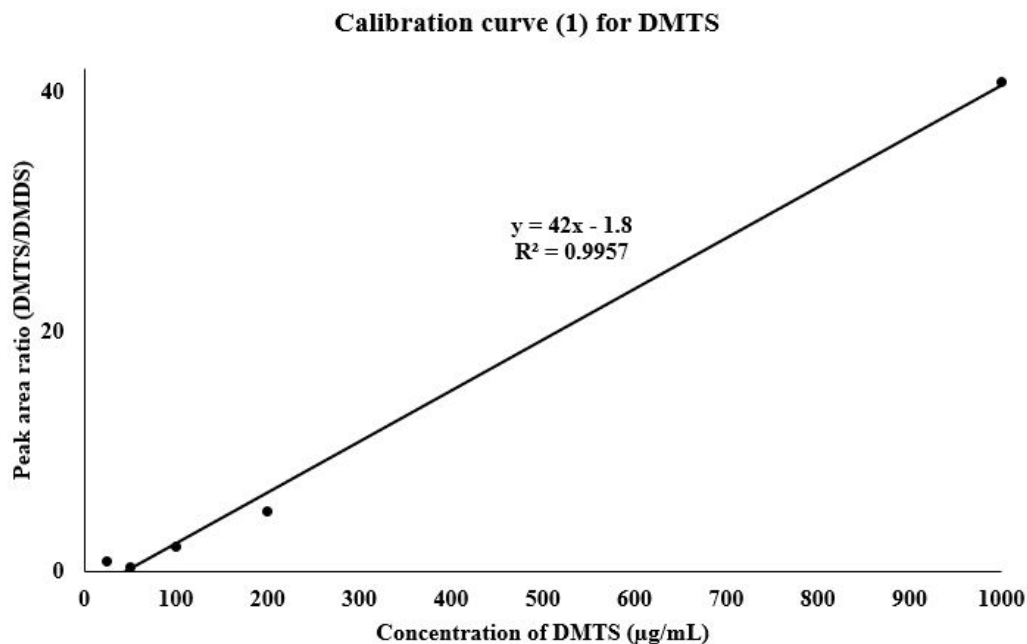


Figure 30. Calibration Curve (1) Observed for DMTS. Data are presented as mean \pm S.D., $n = 2$. The error bars are not visible as the S.D. is low.

The limit of detection (LOD) and limit of quantification (LOQ) were determined for the calibration curve.

$$LOD = y_{blank} + 3s = 0.000 + (3 \times 0.098) = 0.294$$

$$Concentration\ LOD = 3s/m = (3 \times 0.098) / 42 = 0.007\ mg/mL$$

$$LOQ = y_{blank} + 10s = 0.000 + (10 \times 0.098) = 0.980$$

$$Concentration\ LOQ = 10s/m = (10 \times 0.098) / 42 = 0.023\ mg/mL$$

Where y_{blank} is the mean of the blank signal, s is the standard deviation of the signal for the lowest analyzed concentration and m is the gradient of the calibration curve.

$$s = \sqrt{\frac{(x_m - x_i)^2}{n-1}}$$

where x_m is the mean of the repeats, x_i is the individual value of

measurement and n is the number of repeats for the lowest analyzed concentration. The above calibration curve 1 was used to analyze DMTS-F1 in the PAMPA system.

Only the DMTS-F1 diluted with BSB was used in the first PAMPA analysis to determine the permeability. The results showed that DMTS should penetrate the blood brain barrier according to the PAMPA model. At the beginning the acceptor wells did not contain DMTS. For the first 30 min the DMTS concentration increased linearly in the acceptor phase (Figure 31), while in the donor phase it decreased linearly (Figure 32). After 30 min it reached the equilibrium concentration and stayed constant in both compartments. The lipid membrane showed very high DMTS retention (DMTS concentration lost from the donor phase that ended up in the membrane) (Figure 33), determined by the following equation:

$$\text{Membrane retention after incubation} = [\text{DMTS}] \text{ in the donor wells before incubation} - ([\text{DMTS}] \text{ in the acceptor wells after incubation} + [\text{DMTS}] \text{ in donor wells after incubation})$$

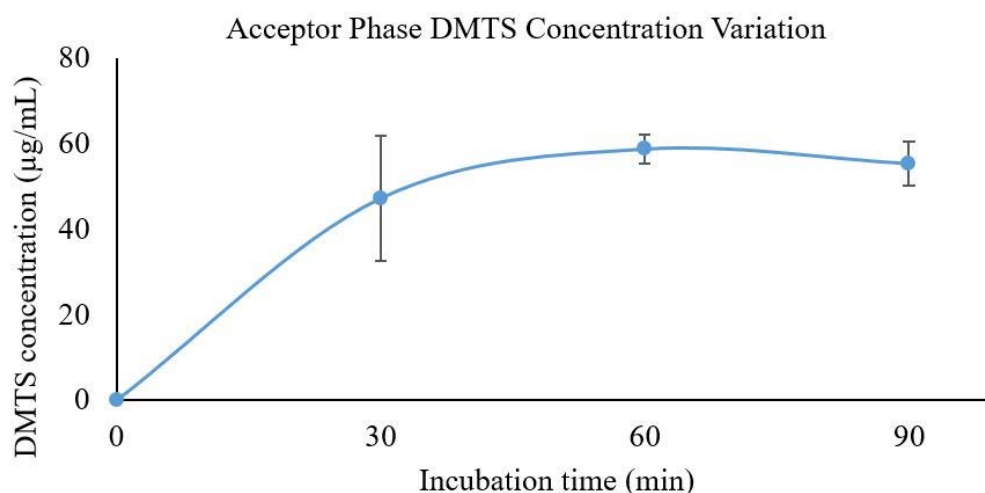


Figure 31. DMTS Concentration Variation in the Acceptor Wells. Samples were analyzed by HPLC-UV and the concentrations were determined by the calibration equation of $y = 37.965x - 0.8897$. Data are presented as mean \pm S.D., $n = 3$. In excel a trendline was added for visual effect.

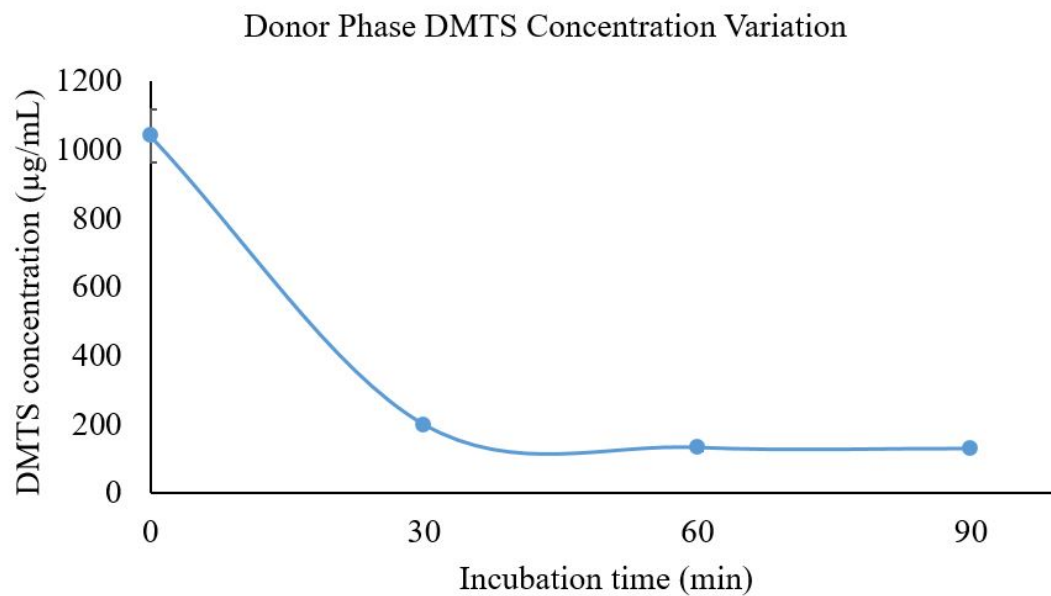


Figure 32. DMTS Concentration Variation in the Donor Wells. Samples were analyzed by HPLC-UV and the concentrations were determined by the calibration equation of $y = 37.965x - 0.8897$. Data are presented as mean \pm S.D., $n = 3$. The error bars are not visible as the S.D. is low.

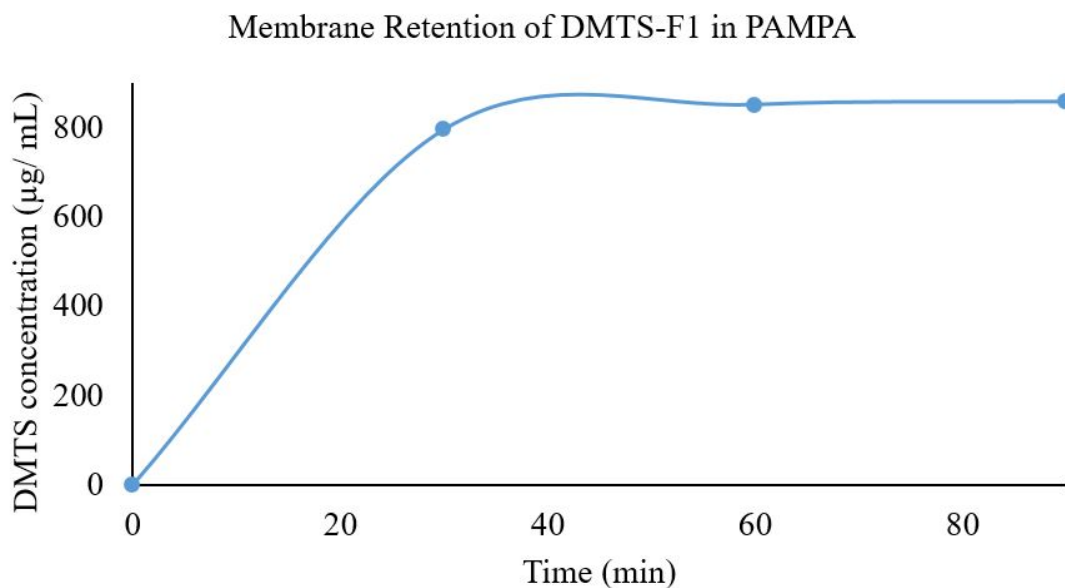


Figure 33. Membrane Retention for DMTS-F1. The DMTS concentration lost from the donor phase (that ended up in the membrane) increased until 30 min and then became constant. DMTS concentration on the y axis shows the DMTS concentration loss from the donor phase.

Calibration curve 2 and comparison of the BBB penetration of two DMTS formulations

The next PAMPA experiment was carried out to compare the BBB penetrability of DMTS-F1 and DMTS-F2. A new calibration curve was built up to analyze the DMTS concentrations. After the sequence run was completed, the results were analyzed by the HPLC software. Peak area ratios of DMTS/DMDS were plotted against DMTS concentrations. Figure 34 shows the of the calibration curve with an R^2 value of 0.9917. The equation of the plot was $y = 0.063x - 0.9$.

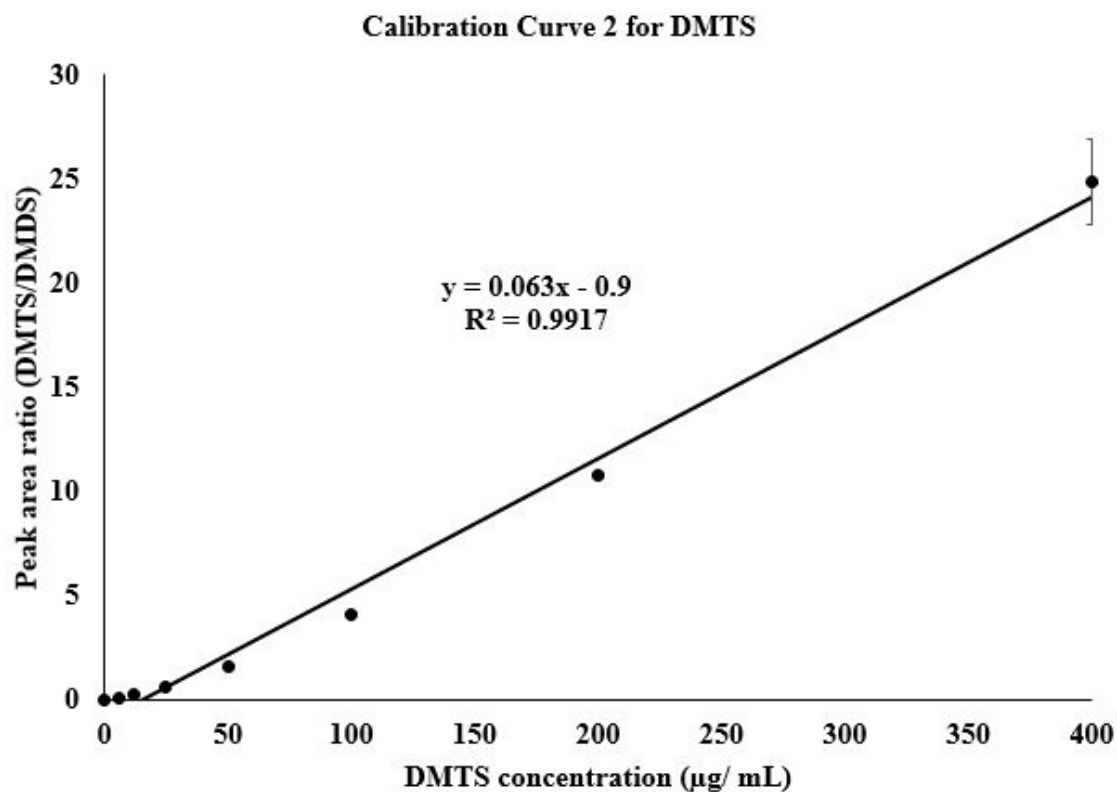


Figure 34. Calibration Curve (2) for DMTS. Data are presented as mean \pm S.D., $n = 3$. Some error bars are not visible as the S.D. is low.

$$LOD = y_{blank} + 3s = 0.009 + (3 \times 0.002) = 0.015$$

$$Concentration\ LOD = 3s/m = (3 \times 0.002)/0.063 = 0.1\ \mu\text{g}/\text{mL}$$

$$LOQ = y_{blank} + 10s = 0.009 + (10 \times 0.002) = 0.029$$

$$Concentration\ LOQ = 10s/m = (10 \times 0.002)/0.063 = 0.3\ \mu\text{g}/\text{mL}$$

Where y_{blank} is the mean of the blank signal, s is the standard deviation of the signal for the lowest analyzed concentration and m is the gradient of the calibration curve.

$$s = \sqrt{\frac{(x_m - x_i)^2}{n-1}}$$

where x_m is the mean of the repeats, x_i is the individual value of

measurement and n is the number of repeats for the lowest analyzed concentration.

The above calibration curve shows a nonlinear relationships below the 0.05 mg/mL concentration point. However, it was approximated as two different linear relationships for DMTS concentration determination in following experiments. The calibration curve was divided into two calibration curves, below 50 $\mu\text{g}/\text{mL}$ (Figure 35) and above 50 $\mu\text{g}/\text{mL}$ (Figure 36).

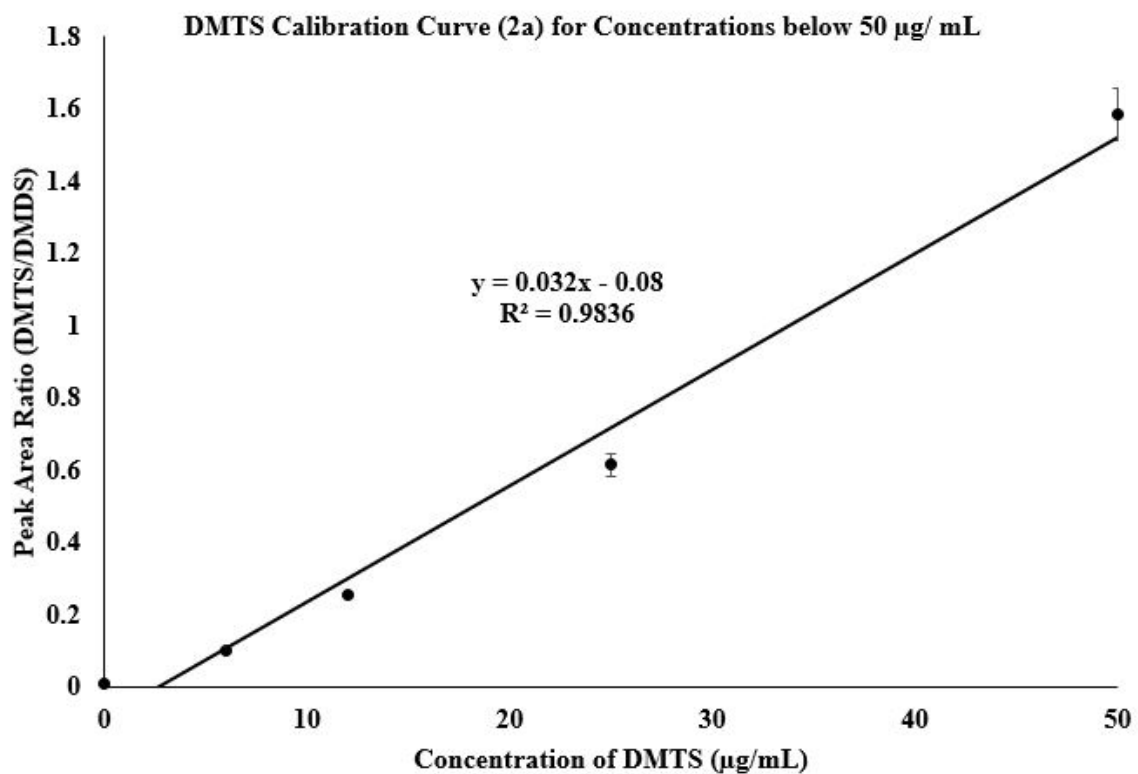


Figure 35. DMTS Calibration Curve (2a) for Concentrations below 0.05 mg/mL. Data are presented as mean \pm S.D., $n = 3$. Some error bars are not visible as the S.D. is low. This curve was used to determine the DMTS concentrations in the acceptor wells of the PAMPA system.

$$LOD = y_{blank} + 3s = 0.009 + (3 \times 0.002) = 0.015$$

$$\text{Concentration } LOD = 3s/m = (3 \times 0.002)/0.032 = 0.2 \mu\text{g}/\text{mL}$$

$$LOQ = y_{blank} + 10s = 0.009 + (10 \times 0.002) = 0.029$$

$$\text{Concentration } LOQ = 10s/m = (10 \times 0.002)/0.032 = 0.9 \mu\text{g}/\text{mL}$$

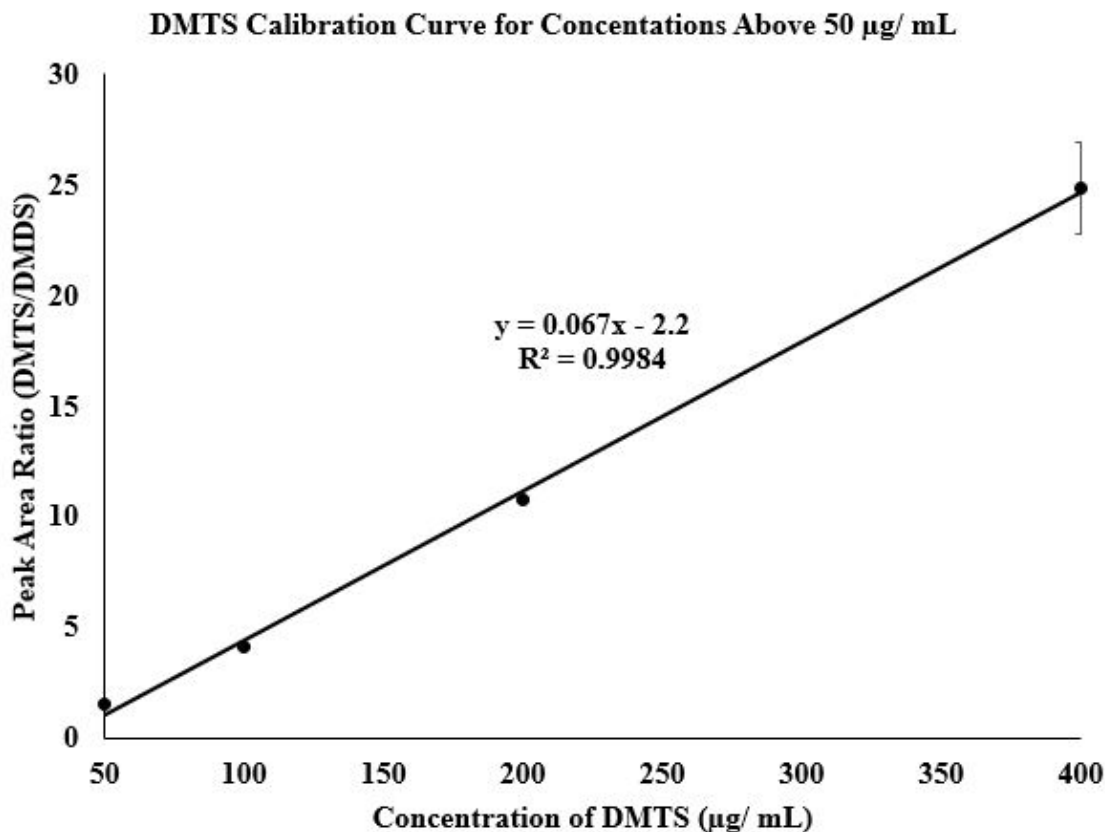


Figure 36. DMTS Calibration Curve (2b) for Concentrations Above 0.05 mg/mL. Data are presented as mean \pm S.D., $n = 3$. Some error bars are not visible as the S.D. is low. This curve was used to determine the DMTS concentrations in the donor wells of the PAMPA system.

$$LOD = y_{blank} + 3s = 0.009 + (3 \times 0.072) = 0.225$$

$$\text{Concentration } LOD = 3s/m = (3 \times 0.072)/0.067 = 3 \mu\text{g/mL}$$

$$LOQ = y_{blank} + 10s = 0.009 + (10 \times 0.072) = 0.729$$

$$\text{Concentration } LOQ = 10s/m = (10 \times 0.072)/0.067 = 11 \mu\text{g/mL}$$

BBB Penetration Determination of DMTS in Two Formulations by the PAMPA System

Permeability of the two DMTS formulations through the PAMPA membrane was determined. Samples from the donor and the acceptor wells were analyzed by HPLC using the calibration curve shown in Figure 37 and Figure 38 respectively. During first the 30

min the amount of DMTS that reached the acceptor phase was much higher for F1, but after 40 min F2 showed higher concentration of DMTS in the acceptor wells.

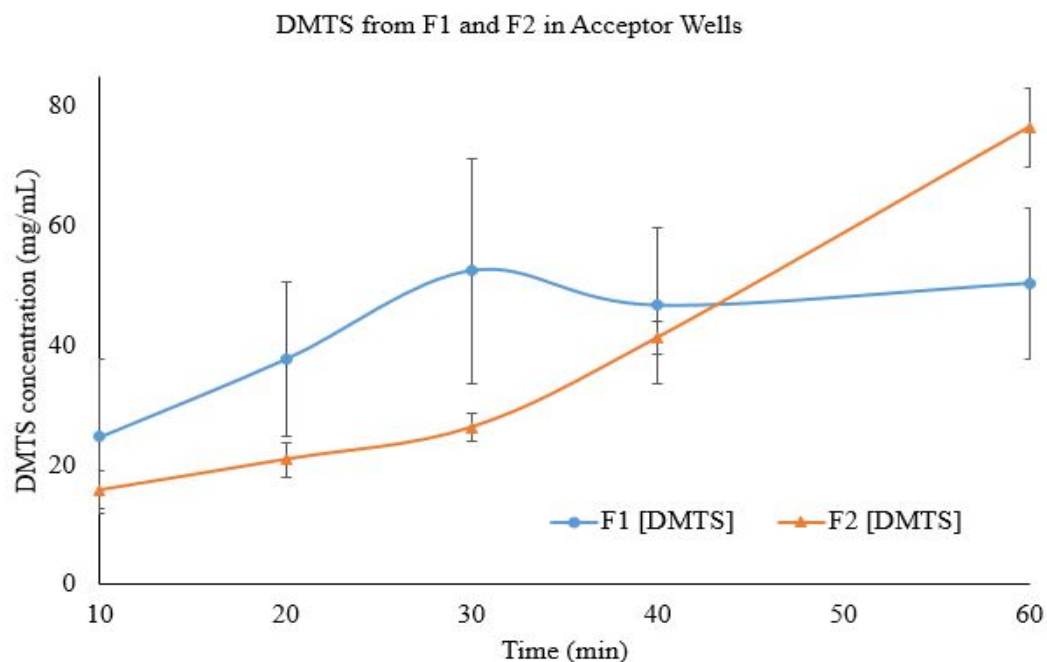


Figure 37. Overlay of DMTS Concentrations in the Acceptor Phase of the PAMPA system for DMTS-F1 and DMTS-F2. Within the first 40 min the DMTS concentration in the acceptor phase for F1 is higher than for F2. Data are presented as mean \pm S.D., $n = 3$.

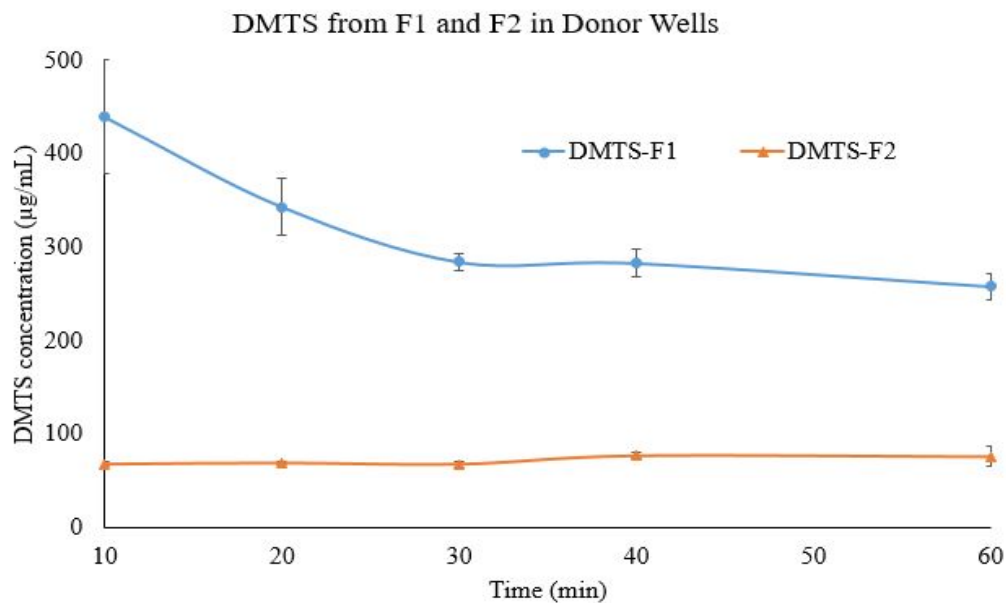


Figure 38. DMTS Concentration from DMTS-F1 and DMTS-F2 in the Donor Phase of the PAMPA. In the donor wells, the concentration of DMTS from F2 is remained below

0.1 mg/ml. Data are presented as mean \pm S.D., n = 3. Some error bars are not visible as the S.D. is low.

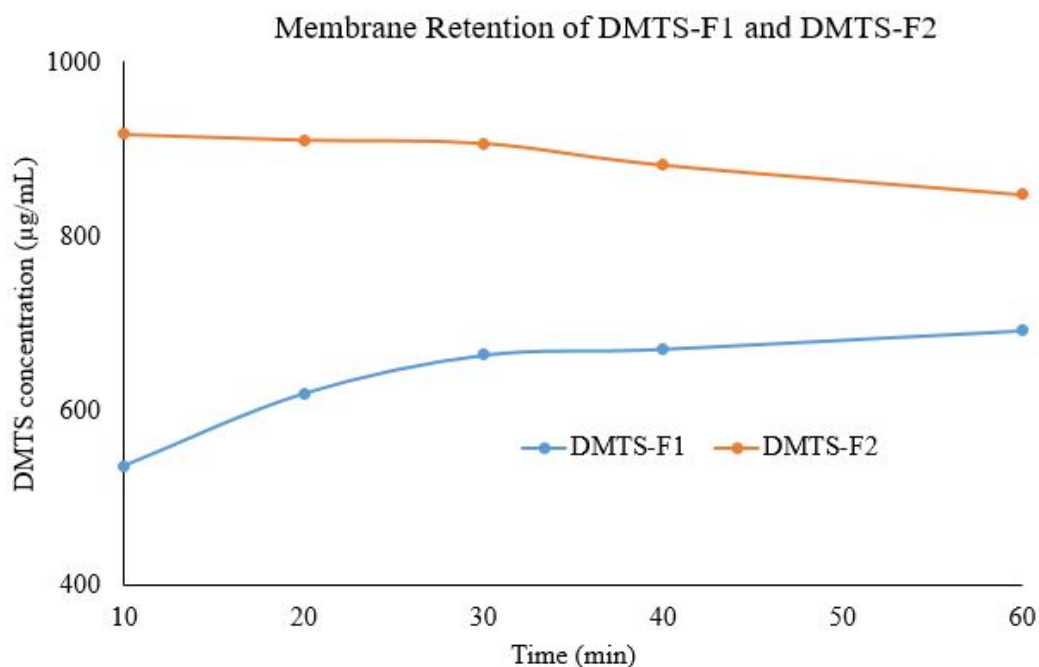


Figure 39. Membrane Retention from DMTS-F1 and DMTS-F2 in the Acceptor Phase of the PAMPA System. DMTS from F2 shows a high concentration at each sampling time.

DMTS from F2 shows lower concentrations in both phases. It was concluded that the DMTS-F2 have much higher tendency to stay in the lipid membrane than F1 (Figure 39). CN is a fast acting poison which needs to be treated fast. Based on the results a formulation which have faster BBB penetration will be more suitable as a CN antidotal drug in the brain. Therefore, DMTS-F1 is superior in crossing the BBB as a CN antidote.

Determining the Effect of Poly80 on the DMTS Permeability for DMTS-F1 in the PAMPA System

The PAMPA acceptor phase contains brain sink buffer at pH 7.4. The solubility of DMTS in aqueous solutions is very low (0.15 mg/mL).⁴⁸ Therefore, the preliminary PAMPA experiments were carried out in the presence of poly80 in the acceptor wells. The

purpose of this study was to confirm the permeability of DMTS-F1 through the membrane in the absence and in the presence of the surfactant in the acceptor phase. Samples were analyzed in HPLC-UV.

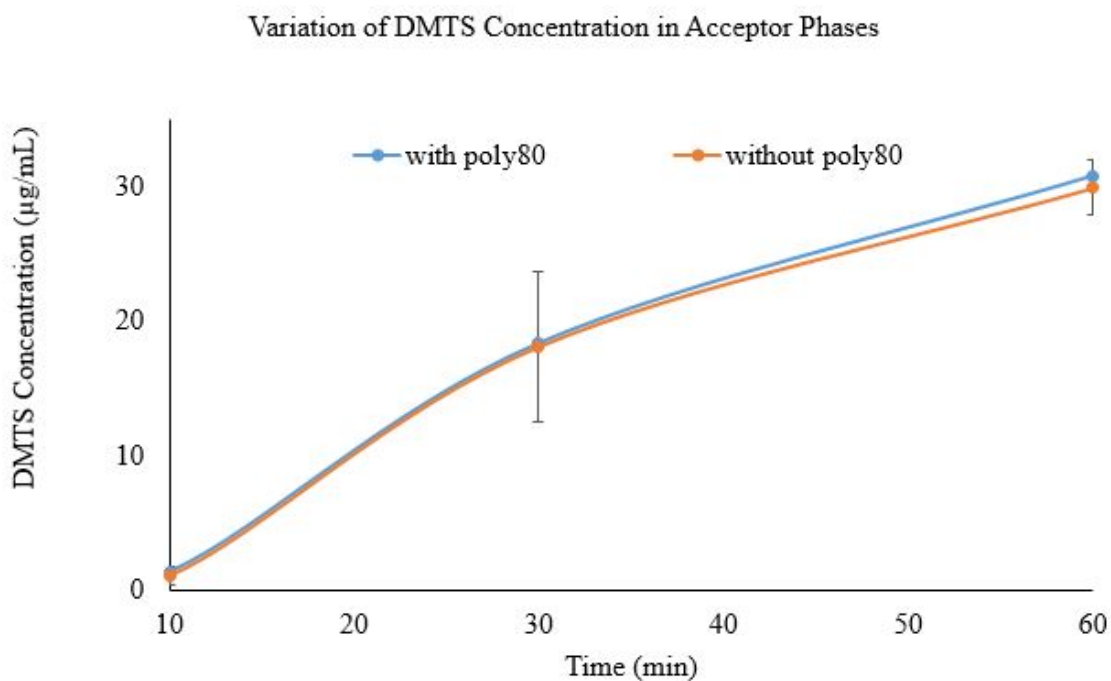


Figure 40. Effect of poly80 to the DMTS Concentration in the Acceptor Phase. Samples were analyzed by HPLC-UV to determine the DMTS concentrations. Data are presented as mean \pm S.D., $n = 3$.

Within the first 30 min the DMTS concentration in the acceptor phase increased rapidly and then the rate of increase was lower. The donor phase concentration decreased with time which was much faster in the first 10 min. The results for two phases are shown in Figure 40 and Figure 41. Most importantly, none of the phases showed any changes in the DMTS concentrations in the presence of the poly80 over the period of the measurement.

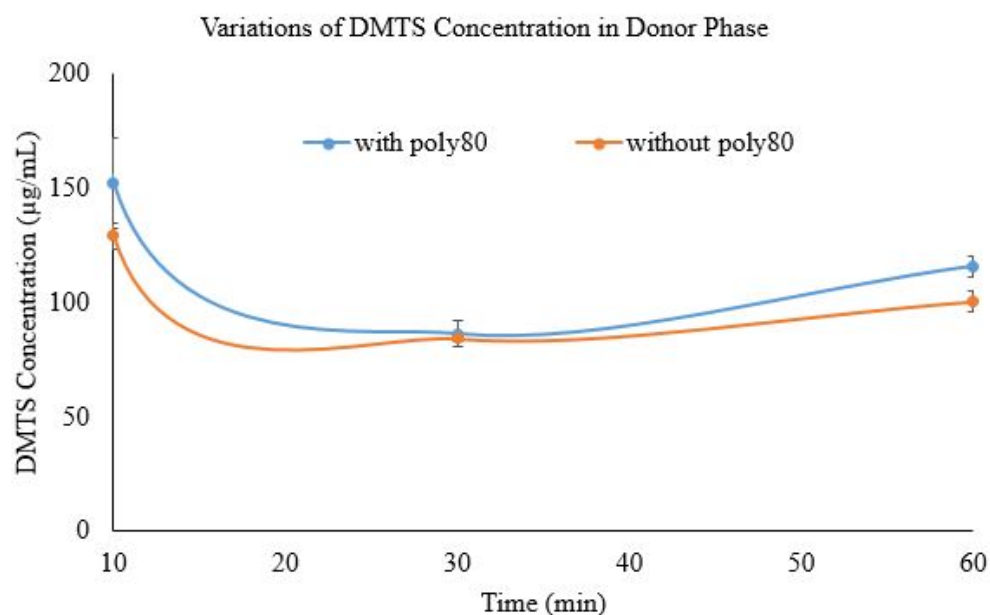


Figure 41. Effect of poly80 to the DMTS Concentration in the Donor Phase. Samples were analyzed for DMTS concentrations by HPLC-UV. Data are presented as mean \pm S.D., $n = 3$. The error bars are not visible as the S.D. is low.

Determining the Effect of the Number of Stirrers on the DMTS Permeability for F1 in the PAMPA System

The BBB conditions are better modelled when stirrers are present only in the donor wells. The purpose of this analysis was to see the effect of the number and the position of stirrers in the PAMPA system. As a reference, another set of wells were incubated without stirrers in both phases. After the incubation was completed, the solution in each well was analyzed by HPLC-UV. The results are shown in Figure 42 and Figure 43.

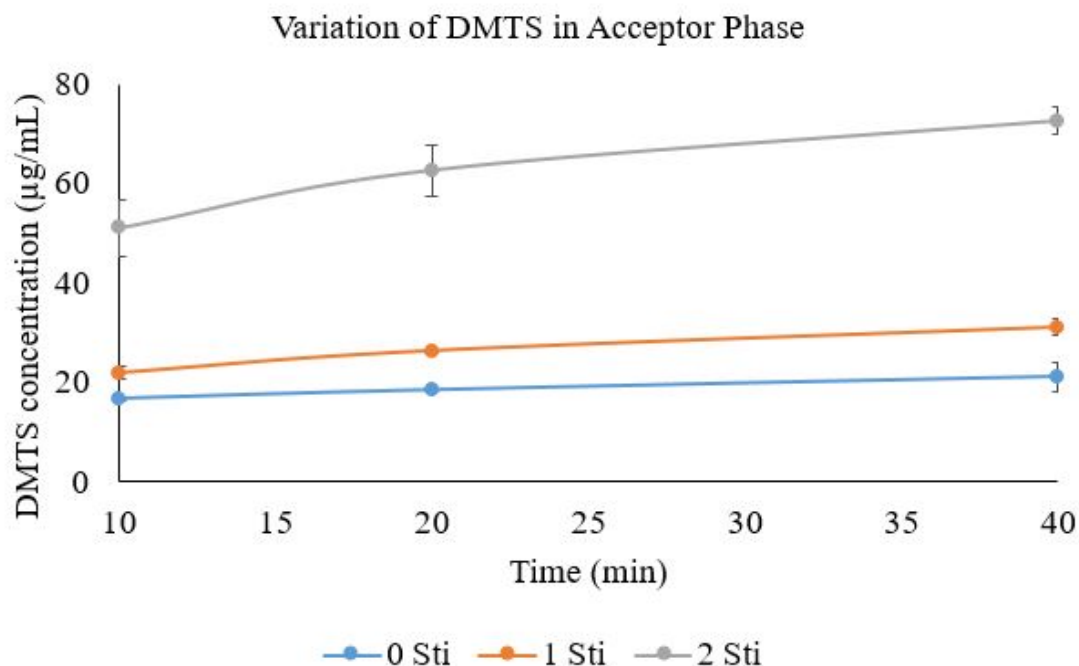


Figure 42. DMTS Concentration in the Acceptor Phase with Different Number of Stirrers. Samples were analyzed for DMTS concentrations by HPLC-UV. Data are presented as mean \pm S.D., $n = 3$. Some error bars are not visible as the S.D. is low.

The DMTS concentration in the acceptor phase increased in the following order: without stirrers (0 Sti), one stirrer in the donor phase (1 Sti) and one stirrer in the donor and one in the acceptor phase (2 Sti). The DMTS concentration in the donor phase was the highest for the unstirred wells in all setups. The DMTS concentration in the donor phase was not significantly different in the 1 Sti and 2 Sti setups. However, the numbers of stirrers did affect the concentration in the more important acceptor wells. This means the three different stirrer conditions resulted in different permeability. Therefore, the number of stirrers were kept constant (1 Sti) in all subsequent studies to achieve comparable results.

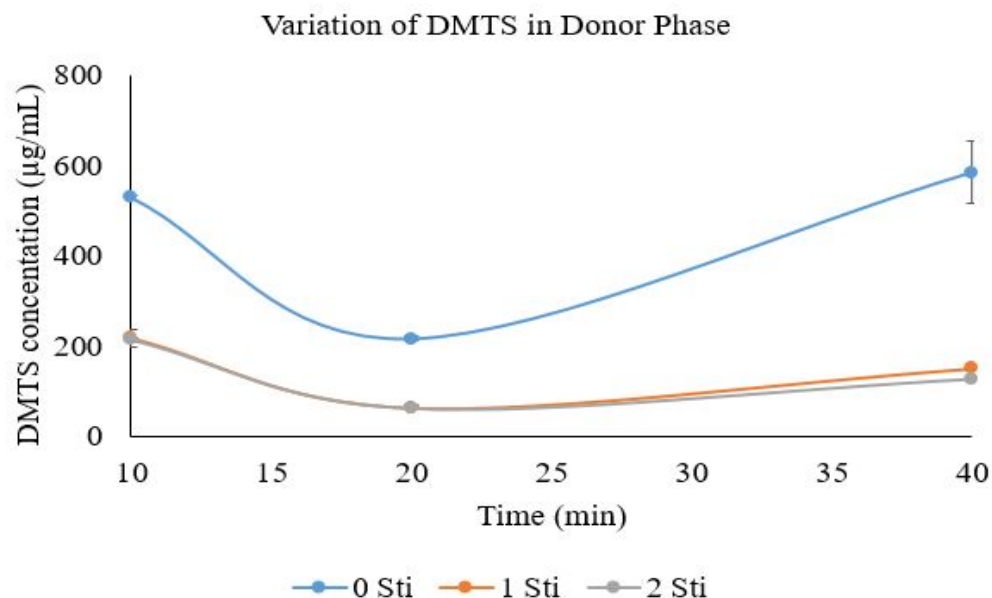


Figure 43. DMTS Concentration in the Donor Phase with Different Number of Stirrers. Samples were analyzed for DMTS concentrations by HPLC-UV. Data are presented as mean \pm S.D., $n = 3$. Some error bars are not visible as the S.D. is low.

Viscosity Determination of the Two Dispersants of the DMTS Formulations

The viscosities of the two dispersion medias used to formulate DMTS were determined using the dropping ball viscometer. The dispersion media of the poly80 formulation (F1), 15% poly80 in deionized water, gave a viscosity of 2.32 cP. Dispersion media F2, the mixture of poly80 and span80, gave a viscosity of 511.00 cP. The experimetal data and calculations are shown in Table 3. The purpose of this study was to collect the viscosity data of the two DMTS formulations for future size distribution studies.

Table 3

Viscosity Calculation for DMTS-F1 and DMTS-F2

Parameter	F1 dispersant media	F2 dispersant media
Composition	15% poly80 and 85% water	25% span80 and 75% poly80
Liquid portion Mass (g)	9.79	7.65
Volume of the liquid portion (mL)	9.80	7.30
Density (ρ) (g/mL)	$\frac{9.79 \text{ g}}{9.80 \text{ mL}} = 1.00$	$\frac{7.65 \text{ g}}{7.30 \text{ mL}} = 1.05$
Density of the metal ball (ρ_0) (g/mL)	8.02	8.02
Time elapsed for travel (s)	8.83	1884.66
Temperature (°C)	25.0	23.2
k	0.0375	0.0389
Viscosity (η) (cP)	$k (\rho_0 - \rho) t$ $= 0.0375 (8.02 - 1.00) 8.83$ $= 2.32$	$k (\rho_0 - \rho) t$ $= 0.0389 (8.02 - 1.05) 1884.67$ $= 511.00$

Droplet Size Distribution of DMTS-F1 Using DLS Instrument

Droplet size distribution of the DMTS-F1 formulation was determined by the DLS instrument (Zetasizer Nano ZS). The viscosity value of the F1 dispersant media (2.32 cP), measured by dropping ball viscometer in the previous section, was used as one of the instrument setup parameters. The size distribution of F1 has been measured periodically since the preparation of the formulation. At the time of writing, it has been 60 days and the measurements are continuing. The droplet sizes of the stock solution measured immediately after the preparation are shown in Table 2 and Figure 14.

Most the droplets (82% of total peak intensity) have an average size of 7 nm. The rest of the particles have the average diameter of 50 nm (17%) and 2796 nm (1 %). After this measurement, the stock solution was crimp-sealed in 2 mL glass vials. Then they were divided into three groups (16 vials in each group) and each were stored in a sealed container at 4°C, 25°C and 37°C, as described in the Figure 44. After an hour, another measurement was carried out by taking samples from vials in the three different temperature groups. The results are shown in Table 4 and Figure 45.

Sampling time intervals were 1 hour, 2 hours, 3 hours, 1 day, 2 days, 3 days, 1 week, 2 weeks, 3 weeks, 1 month, 2 months, 3 months, and 6 months. At each time point listed above, one vial from each temperature group were taken and measured by the DLS instrument three times each.

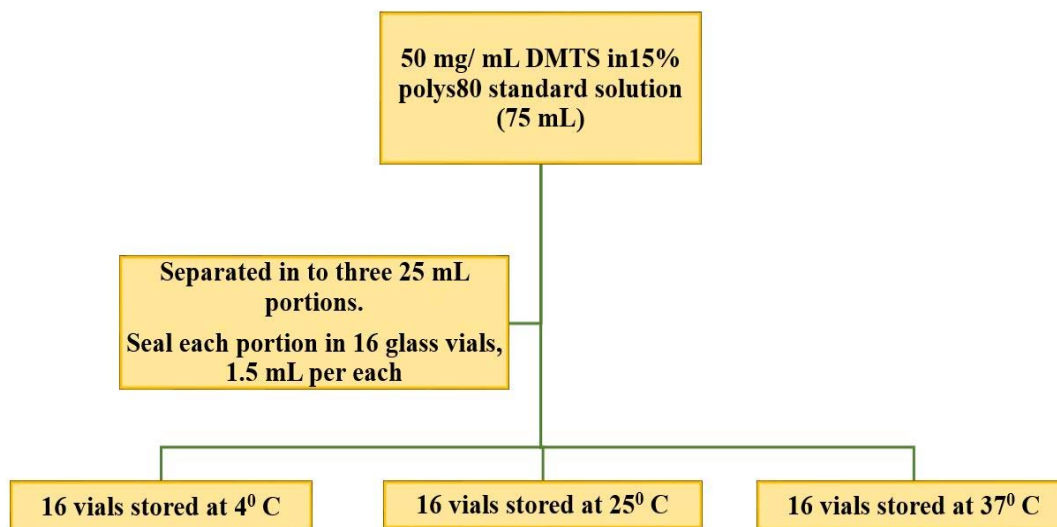


Figure 44. Distributing the DMTS-F1 Stocks Solution to Three Different Temperature Groups. One vial was taken out at each sampling time and analyzed for size distribution.

Table 4

Average Droplet Size Results for the DMTS-F1 Samples Stored at 4 °C, 25 °C and 37 °C for One Hour After the Preparation

Peak	4°C	25°C	37°C
Peak 1	7 (77%)	8 (83%)	7 (75%)
Peak 2	55 (21%)	55 (16%)	39 (24%)
Peak 3	2875 (2%)	1488 (1%)	3026 (1%)

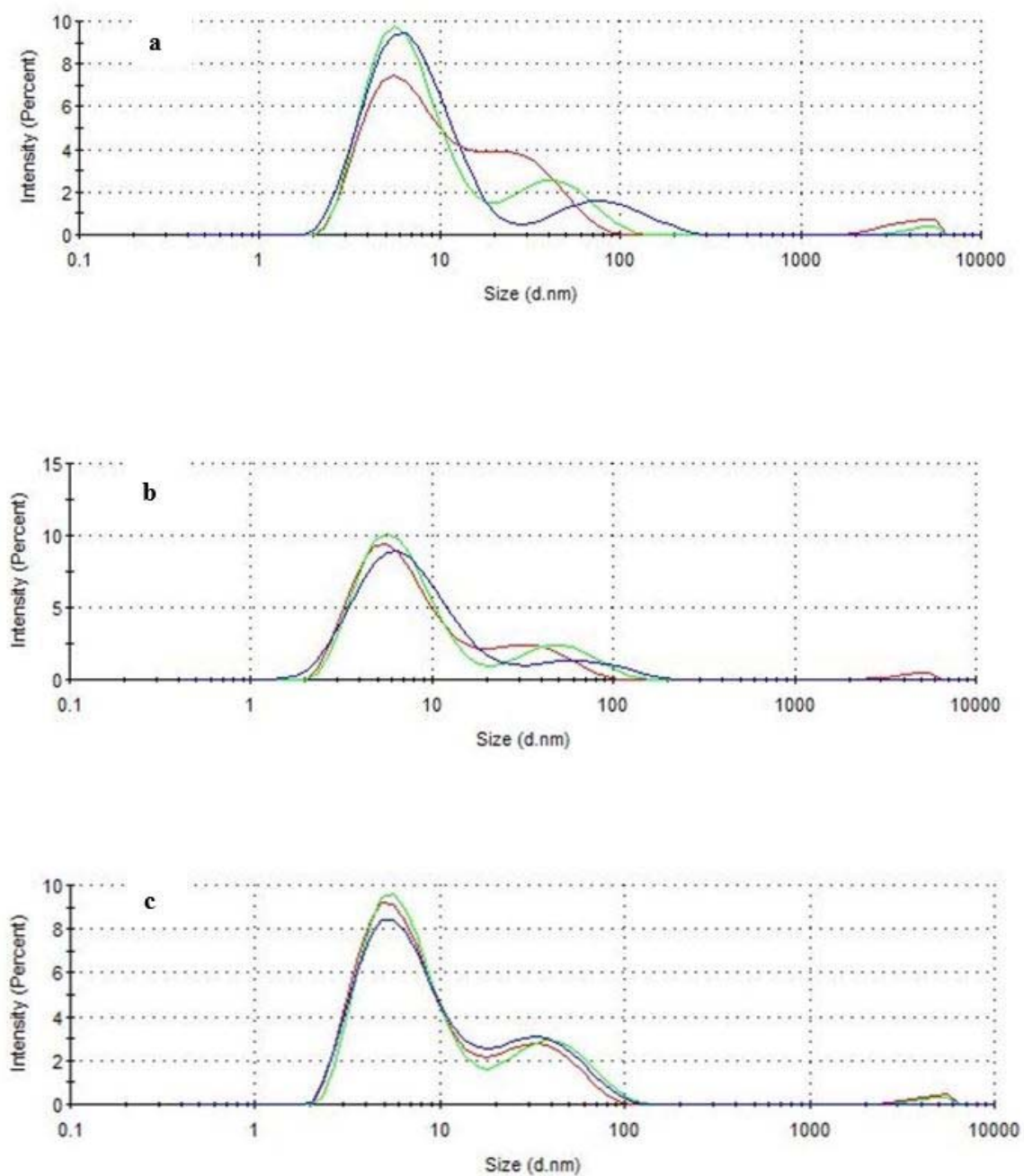


Figure 45. Size Distribution of the DMTS-F1 One Hour After Preparation. a) at 4°C b) at 25°C c) at 37°C. The particle sizes in the DMTS-F1 stored for one hour in all three temperatures did not show a level of change that indicated instability that would cause a problem in downstream applications. The red, green and blue lines represent the three measurements for the same sample.

After one hour, the DMTS-F1 samples showed very similar size distribution stored at all three temperatures. Analysis was continued for 60 days by following the same method described above. Figure 46 to Figure 48 shows the change of the major droplet size and the major droplet percentage with the sampling time.

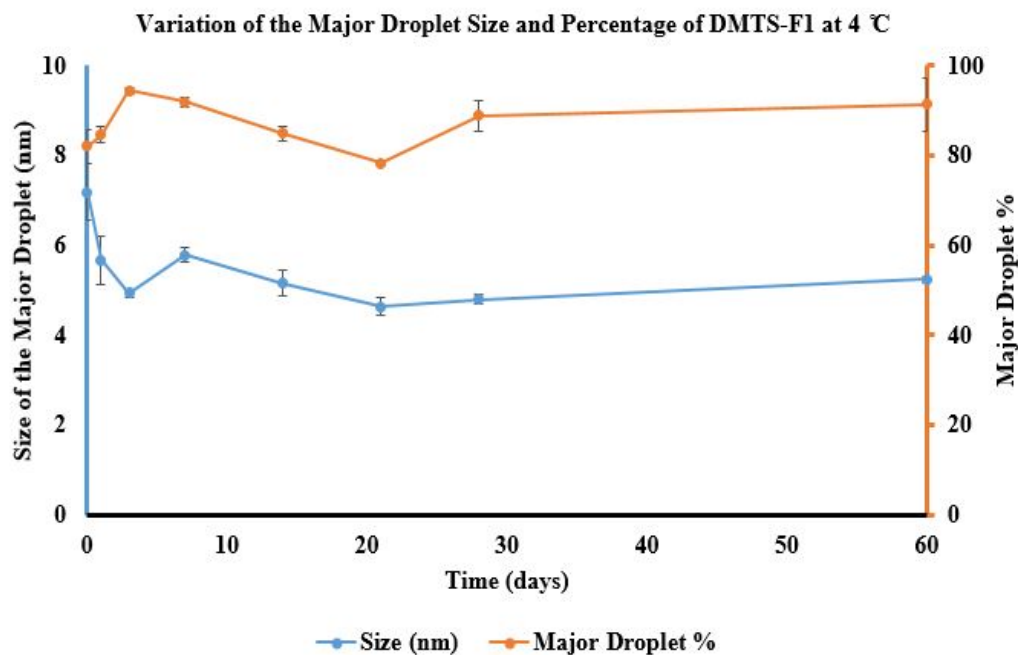


Figure 46. Major Droplet Size and the Percentage Variation with Sampling Time for DMTS-F1 at 4 °C. Data are presented as mean \pm S.D., $n = 3$. The error bars are not visible for some data points as the S.D. is low.

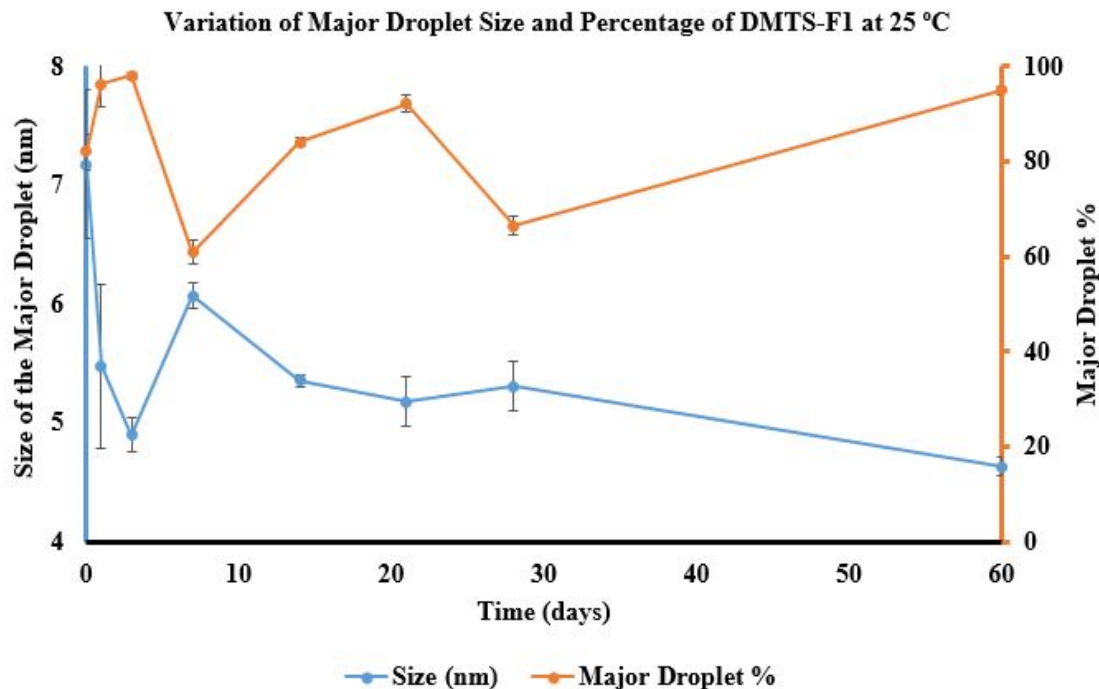


Figure 47. Major Droplet Size and the Percentage Variation with Sampling Time for DMTS-F1 at 25 °C. Data are presented as mean \pm S.D., n = 3. Some error bars are not visible as the S.D. is low.

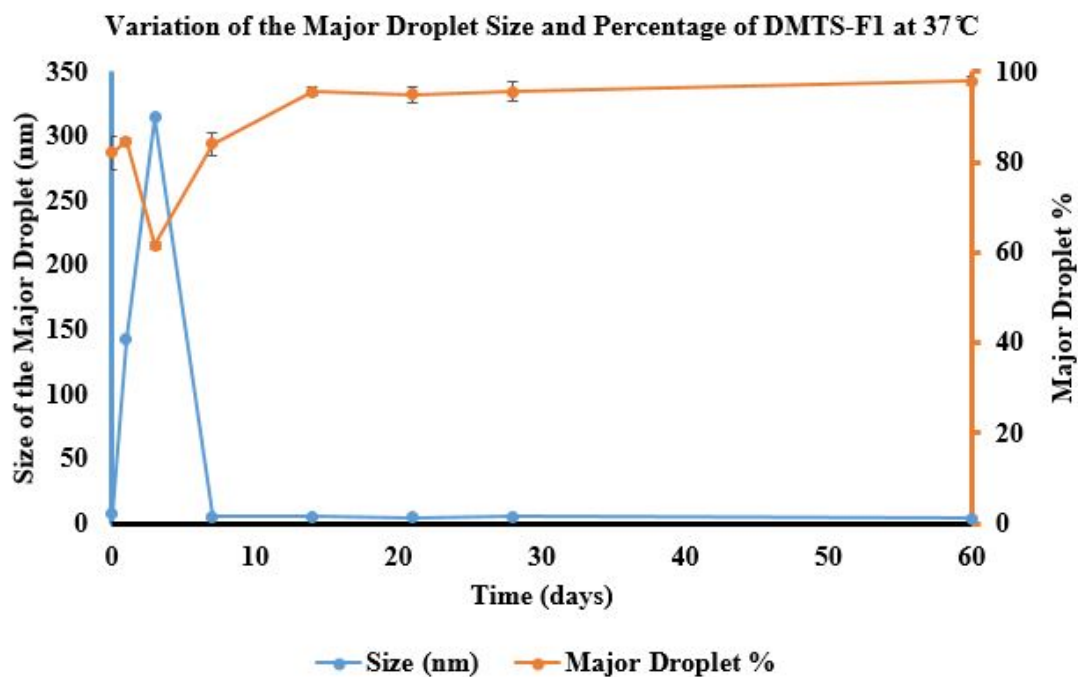


Figure 48. Major Droplet Size and the Percentage Variation with Sampling Time for DMTS-F1 at 37 °C. Data are presented as mean \pm S.D., n = 3. The error bars are not visible as the S.D. is low.

The results show that particle sizes in the samples maintained at 4 °C and 25 °C have negligible variation throughout the sixty days of analysis: in each case, the majority of the particles were below 10 nm. In each case the percentage of the most abundant droplet size was higher than 60% (Figure 46 and Figure 47). These results suggested that the DMTS-F1 can be stored at either 4 °C or 25 °C without a change in the droplet size distribution. Samples stored under 37 °C showed different results: the droplet sizes increased by the second and third day. However, after seven days the droplet size dropped back to less than 10 nm. This may be because in F1 the droplets sizes are more stable below 10 nm. In the future, more frequent sampling within the first seven days will be performed to understand the dynamic changes in droplet size distribution. In the F2 dispersant media, the very high viscosity value of 510 cP makes it impossible to measure the droplet sizes by the DLS method.

Analytical Method Development to Determine DMTS in Blood Samples, Collected During Pharmacokinetics Studies, by Using HPLC.

The peak area ratios for DMTS concentrations (0, 1, 2, 4 and 8 µg/ mL) gave a linear calibration curve with an R^2 of 0.9975 and an equation of $y = 0.0077x + 0.0014$ (Figure 49). This calibration curve was used to analyze samples for the pharmacokinetic studies.

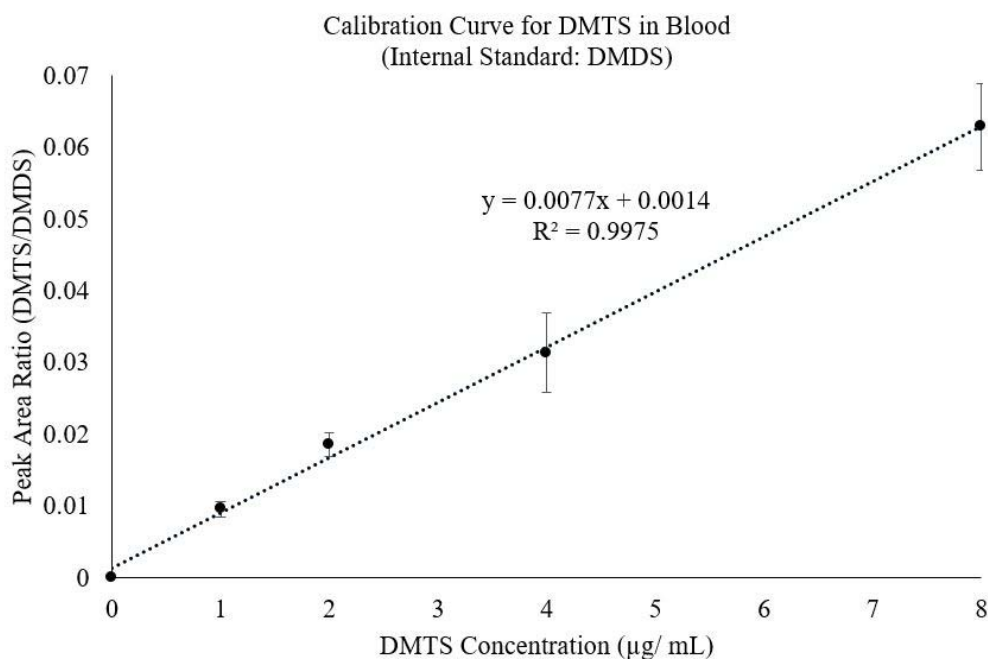


Figure 49. Calibration Curve for DMTS in Blood. Data are presented as mean \pm S.D., $n =$

3. The limit of detection (LOD) and the limit of quantification (LOQ) were determined based on the following calculations:

$$LOD = y_{blank} + 3s = 0.000 + (3 \times 0.001) = 0.001$$

$$Concentration\ LOD = 3s/m = (3 \times 0.001) / 0.0077 = 0.4\ \mu\text{g}/\text{mL}$$

$$LOQ = y_{blank} + 10s = 0.000 + (10 \times 0.001) = 0.010$$

$$Concentration\ LOQ = 10s/m = (10 \times 0.001) / 0.0077 = 1.3\ \mu\text{g}/\text{mL}$$

Where y_{blank} is the mean of the blank signal, s is the standard deviation of the signal for the lowest analyzed concentration and m is the gradient of the calibration curve.

$s = \sqrt{\frac{(x_m - x_i)^2}{n-1}}$ where x_m is the mean of the repeats, x_i is the individual value of the measurement and n is the number of repeats for the lowest analyzed concentration.

Pharmacokinetics of DMTS-F1 and DMTS-F2

Samples from each incubation time were analyzed according to the previously explained method using HPLC-UV. Both formulations were injected in the same dose, 150 mg/ kg. The DMTS concentrations vs. incubation time were plotted as shown in Figure 50 and Figure 51 below.

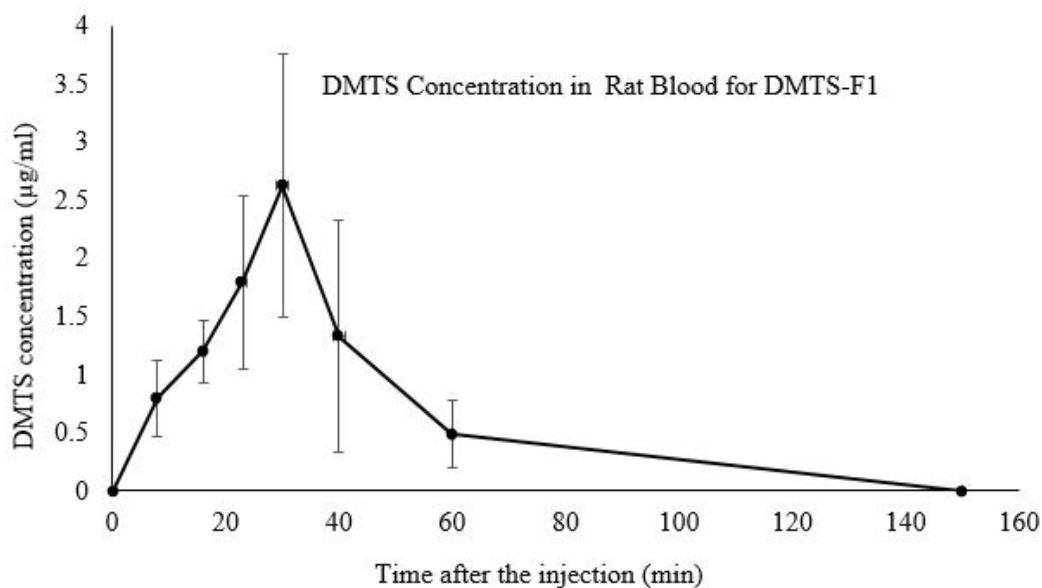


Figure 50. DMTS Concentration in Rat Blood for DMTS-F1. Data are presented as mean \pm S.D., $n = 2$. DMTS concentrations were determined using the HPLC-UV.

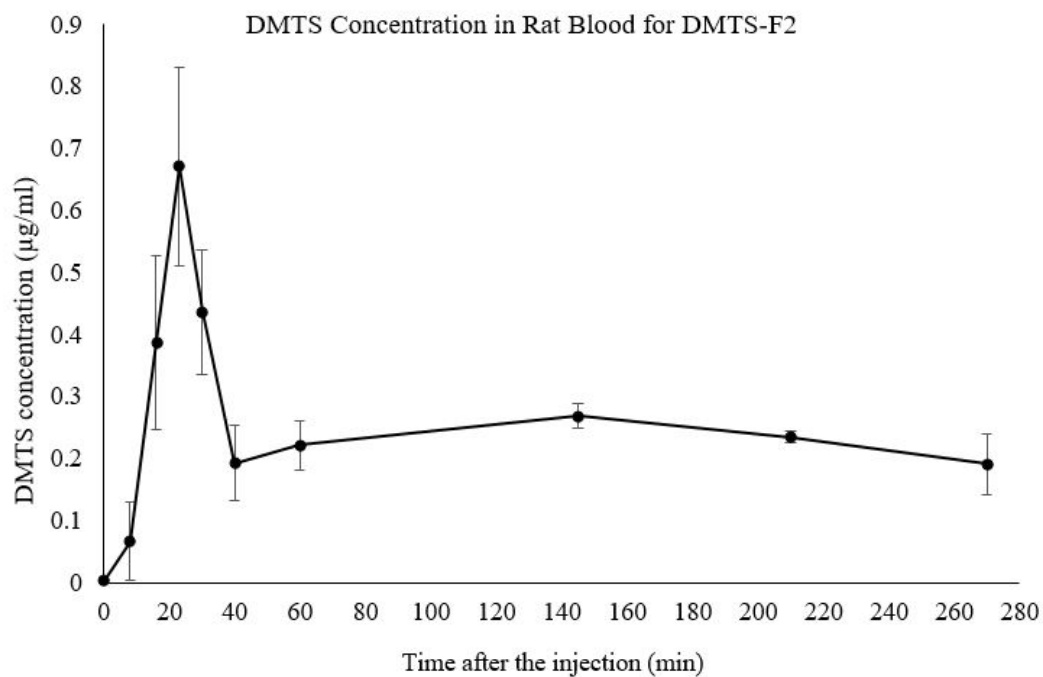


Figure 51. DMTS Concentration in Rat Blood for DMTS-F2. Data are presented as mean \pm S.D., $n = 2$. DMTS concentrations were determined using the HPLC-UV.

Three male CD rats were used for each formulation to determine the absorption kinetics. Both DMTS-F1 and DMTS-F2 provided the highest DMTS concentrations in the range of 23 to 30 min. For F1 the highest concentration in the rat blood was 2.62 $\mu\text{g/mL}$ and for F2 it was only 0.37 $\mu\text{g/mL}$. These results suggest that DMTS-F1 provides higher DMTS concentration into the circulation.

CHAPTER IV

CONCLUSION

Analytical Method Development for CN, TS and NT by Using IC

CN is a naturally occurring toxic compound that has been used as a chemical weapon. TS and NT are the two components of one of the present CN therapeutics, Nithiodote™. In Dr. Petrikovics's lab, different ongoing *in-vivo* and *in-vitro* investigations are being carried out with various CN antidote molecules including TS and NT. It is important to determine the concentrations of the CN, NT and TS solutions before they are used in various antidotal studies. The IC methods, developed during this research for NT and TS, are providing rapid analytical determinations. The cost of the solvents for operating an IC is lower than for HPLC, as aqueous solutions are used. Each calibration curve showed high linearity with $R^2 > 0.9900$. As the instrument broke we could not obtain enough data for the TS calibration curve. Further studies will be run after the IC is repaired.

Analytical Method Development for DMTS detection by HPLC-UV

An analytical method to determine the amount of DMTS in the PAMPA system was developed, focusing on the lower concentrations in the PAMPA wells. Calibration curve 2 showed high linearity with an R^2 of 0.9914. However, in this calibration curve the data points below 0.05 mg/mL showed a deviation from the major trend-line. Therefore, the calibration curve was split into two linear parts (calibration curve 2a and 2b). This technique could be used to determine DMTS concentrations in a clear liquid without any major turbidity. The separation of the analyte from blood is harder compared to non-biological samples. Therefore, a second analytical method for DMTS quantitation was developed for blood, where the analyte was extracted by acetonitrile before injection to the

HPLC column (Extraction technique of DMTS to acetonitrile was previously published by Dr. Petrikovics' Lab⁴⁶). This calibration curve was used for the PK studies.

Viscosity and Droplet Size Distribution Kinetics of DMTS-F1 and DMTS-F2

To use DLS the viscosities of the two formulations were measured with a dropping ball viscometer. F1 dispersant media showed a moderate viscosity of 2.32 cP and F2 had a high value of 511.00 cP.

DMTS-F1 showed uniform droplet size distribution right after preparation. Over 70% of all the droplets had the same diameter. The samples kept for two months at 25 °C and 4 °C showed similar size distribution to the freshly prepared samples. However, samples that were stored at 37 °C had a variation in size in the first three days. Therefore, to preserve the droplet sizes for longer time, the samples should be stored at 25 °C or 4 °C.

BBB Penetration of DMTS-F1 and DMTS-F2

The permeability results in the PAMPA system shows that DMTS-F1 has a much higher BBB permeability and a lower membrane retention. This is an advantage for a CN antidote because CN is a fast acting toxic. DMTS-F2 demonstrated high membrane retention. Also, the DMTS concentration received to the acceptor phase from DMTS-F2 was lower than the DMTS-F1 until the first 40 minutes. However, the maximum percent concentration of DMTS that has reached to the brain side from both formulations was less than 10% of the starting concentration.

Pharmacokinetics Study

Pharmacokinetic results showed that the DMTS-F1 is absorbing faster into the circulation and giving higher c_{max} vs. DMTS-F2. The limited solubility of DMTS in poly80 (80 mg/mL) leads to a high injection volume requirement in order to reach the desired dose

of DMTS in the body, and it was necessary to develop a new formulation of F2. The mixture of span80 and poly80 in the F2 formulation can dissolve up to 500 mg of DMTS per 1 mL, consequently decreasing the injection volume dramatically. With this advanced formulation, we expect that in the future DMTS will become a therapeutic drug against CN intoxication.

Future Recommendations

A mathematical function should be developed to optimize the DMTS calibration curve (2) equation. IC analytical method for TS required to be repeated with more calibration standards and replicates. Based on this permeability and kinetic studies, DMTS-F1 formulation looks more practical than DMTS-F2. However, DMTS-F1 has the disadvantage of the lower solubility, consequently requiring higher injection volume to reach the required DMTS dose in the body. A new formulation with the combined advantages of DMTS-F1 and DMTS-F2 seems to be required to be developed.

REFERENCES

- (1) Garrett, R. H.; Grisham, C. M. *Biochemistry*, 3rd ed.; Kiselica, S., Williams, P., White, A., Eds.; Thomson Learning: Belmont, 2005.
- (2) Jensen, P.; Wilson, M. T.; Aasa, R.; Malmström, B. G. Cyanide Inhibition of Cytochrome c Oxidase. A Rapid-Freeze E.p.r. Investigation. *Biochem. J.* **1984**, *224* (3), 829–837.
- (3) Vick, J. A.; Froehlich, L. H. Studies of Cyanide Poisoning. *Arch. Int. Pharmacodyn. Ther.* **1985**, *273* (2), 314–322.
- (4) Petrikovics, I.; Budai, M.; Kovacs, K.; Thompson, D. E. Past, Present and Future of Cyanide Antagonism Research: From the Early Remedies to the Current Therapies. *World J Methodol* **2015**, *5* (2), 88–100.
- (5) Harborne, J. B. *The Chemical Basis of Plant Defense*; Palo, R. T., Robbins, C. T., Eds.; CRC press, Inc: Boca Raton, 1991.
- (6) Zagrobelny, M.; Bak, S.; Olsen, C. E.; Møller, B. L. Intimate Roles for Cyanogenic Glucosides in the Life Cycle of *Zygaena Filipendulae* (Lepidoptera, Zygaenidae). *Insect Biochem. Mol. Biol.* **2007**, *37* (11), 1189–1197.
- (7) Baskin, S. I. Zyklon B. In *The Holocaust Encyclopedia*; Laqueur, W., Baumel, J. T., Eds.; Yale University Press: Yale, 2001; pp 716–719.
- (8) Rockwood, G. A.; Thompson, D. E.; Petrikovics, I. Dimethyl Trisulfide: A Novel Cyanide Countermeasure. *Toxicol. Ind. Heal.* **2016**, *32* (12), 2009–2016.
- (9) Karalliedde, L.; Wheeler, H.; Maclehorse, R.; Murray, V. Possible Immediate and Long-Term Health Effects Following Exposure to Chemical Warfare Agents. *Public Health* **2000**, *114* (4), 238–248.

- (10) Hope Pharmaceuticals. *Nithiodote Prescribing Information Sheet*; 2011.
- (11) Shiva, S. Nitrite: A Physiological Store of Nitric Oxide and Modulator of Mitochondrial Function. *Redox Biol.* **2013**, *1* (1), 40–44.
- (12) Torres, J.; Darley-Usmar, V.; Wilson, M. T. Inhibition of Cytochrome c Oxidase in Turnover by Nitric Oxide: Mechanism and Implications for Control of Respiration. *Biochem. J.* **1995**, *312*, 169–173.
- (13) Leavesley, H. B.; Li, L.; Prabhakaran, K.; Borowitz, J. L.; Isom, G. E. Interaction of Cyanide and Nitric Oxide with Cytochrome c Oxidase: Implications for Acute Cyanide Toxicity. *Toxicol. Sci.* **2008**, *101* (1), 101–111.
- (14) Borron, S. W.; Stonerook, M.; Reid, F. Efficacy of Hydroxocobalamin for the Treatment of Acute Cyanide Poisoning in Adult Beagle Dogs. *Clin. Toxicol. (Phila)*. **2006**, *44*, 5–15.
- (15) Marraffa, J. M.; Cohen, V.; Howland, M. A. Antidotes for Toxicological Emergencies: A Practical Review. *Am. J. Heal. Pharm.* **2012**, *69* (3), 199–212.
- (16) Petrikovics, I.; Baskin, S. I.; Beigeel, K. M.; Schapiro, B. J.; Rockwood, G. A.; Manage, A. B.; Budai, M.; Szilasi, M. Nano-Intercalated Rhodanese in Cyanide Antagonism. *Nano-toxicology* **2010**, *4* (2), 247–254.
- (17) Westley, J. Thiosulfate: Cyanide Sulfurtransferase (Rhodanese). *Method Enzymol.* **1981**, *77*, 285–291.
- (18) Petrikovics, I.; Cannon, E. P.; McGuinn, W. D.; Pei, L.; Pu, L.; Lindner, L. E.; Way, J. L. Cyanide Antagonism with Carrier Erythrocytes and Organic Thiosulfonates. *Fundam. Appl. Toxicol.* **1995**, *24* (1), 86–93.
- (19) Chen, K. K.; Rose, C. L. Nitrite and Thiosulphate Therapy in Cyanide Poisoning.

- JAMA Intern. Med.* **1952**, *149* (2), 113–119.
- (20) Merck Sante. *Cyanokit Product Information- Annex I*; 2009.
- (21) Block, E. The Chemistry of Garlic and Onions. *Sci. Am.* **1985**, *252* (3), 114–119.
- (22) Iciek, M.; Bilaska, A.; Ksiazek, L.; Srebro, Z.; Włodek, L. Allyl Disulfide as Donor and Cyanide as Acceptor of Sulfane Sulfur in the Mouse Tissues. *Pharmacol. Reports* **2005**, *57* (2), 212–218.
- (23) Gijs, L.; Perpète, P.; Timmermans, A.; Collin, S. 3-Methylthiopropionaldehyde as Precursor of Dimethyl Trisulfide in Aged Beers. *J. Agric. Food Chem.* **2000**, *48* (12), 6196–6199.
- (24) Maruyama, F. T. Identification of Dimethyl Trisulfide as a Major Aroma Component of Cooked Brassicaceous Vegetables. *J. Food Sci.* **1970**, *35* (5), 540–543.
- (25) Buttery, R. G.; Guadagni, D. G.; Ling, L. C.; Seifert, R. M.; Lipton, W. Additional Volatile Components of Cabbage, Broccoli, and Cauliflower. *J. Agric. Food. Chem.* **1976**, *24* (4), 829–832.
- (26) Shirasu, M.; Nagai, S.; Hayashi, R.; Ochiai, A.; Touhara, K. Dimethyl Trisulfide as a Characteristic Odor Associated with Fungating Cancer Wounds. *Biosci. Biotechnol. Biochem.* **2009**, *73* (9), 2117–2120.
- (27) Petrikovics, I.; Baskin, S. I.; Rockwood, G. A. Dimethyl Trisulfide as a Cyanide Antidote. US20150290143 A1, 2015.
- (28) Petrikovics, I.; Kovacs, K. Formulations of Dimethyl Trisulfide for Use as a Cyanide Antidote. US9456996 B2, 2015.
- (29) Abbot, N. J.; Rönnbäck, L.; Hansson, E. Astrocytes-Endothelial Interactions at the

- Blood-Brain Barrier. *Nat. Rev. Neurosci.* **2006**, *7*, 41–53.
- (30) Tajés, M.; Ramos-Fernández, E.; Weng-Jiang, X.; Bosch-Morató, M.; Guivernau, B.; Eraso-Pichot, A.; Salvador, B.; Fernández-Busquets, X.; Roquer, J.; J., M. F. The Blood-Brain Barrier: Structure, Function and Therapeutic Approaches to Cross It. *Mol. Membr. Biol.* **2014**, *31* (5), 152–167.
- (31) Wolburg, H.; Lippoldt, A. Tight Junctions of the Blood-Brain Barrier: Development, Composition and Regulation. *Vascul. Pharmacol.* **2002**, *38* (6), 323–337.
- (32) Abbott, N. J. Blood-Brain Barrier Structure and Function and the Challenges for CNS Drug Delivery. *J. Inherit. Metab. Dis.* **2013**, *36* (3), 437–449.
- (33) Rao, A. L.; Sankar, G. G. Caco-2 Cells: An Overview. *JPRHC* **2009**, *1* (2), 260–275.
- (34) Hilgers, A. R.; Conradi, R. A.; Burton, P. S. Caco-2 Cell Monolayers as a Model for Drug Transport across the Intestinal Mucosa. *Pharm. Res.* **1990**, *7* (9), 902–910.
- (35) Veronesi, B. Characterization of the MDCK Cell Line for Screening Neurotoxicants. *Neurotoxicology* **1996**, *17* (2), 433–443.
- (36) Di, L.; Kerns, E. H.; Bezar, I. F.; Petusky, S. L.; Huang, Y.; Sugano, K.; Yamauchi, Y.; Porter, R. A.; Jeffrey, P.; Cianfrogna, J.; et al. Comparison of Blood-Brain Barrier Permeability Assays: In Situ Brain Perfusion, MDR1-MDCKII and PAMPA-BBB. *J. Pharm. Sci.* **2009**, *98* (6), 1980–1991.
- (37) Pion. *Instruction Manual for PAMPA Explorer Permeability Analyzer*; Pion Inc.: Billerica, 2013.
- (38) Avdeef, A. The Rise of PAMPA. *Expert Opin. Drug Metab. Toxicol.* **2005**, *1* (2).

- (39) Ruell, J. Membrane-Based Drug Assays. *Mod. Drug Disc* **2003**, No. January, 28–30.
- (40) Malvern Instruments. *Zetasizer-Nano Series Basic Guide*; Malvern Instruments Ltd: Worcestershire, 2012.
- (41) Kulikov, K. G.; Koshlan, T. V. Measurement of Sizes of Colloid Particles Using Dynamic Light Scattering. *Tech. Phys.* **2015**, *60* (12), 1758–1764.
- (42) Varenne, F.; Botton, J.; Merlet, C.; Hillaireau, H.; Legrand, F. X.; Barratt, G.; Vauthier, C. Size of Monodispersed Nanomaterials Evaluated by Dynamic Light Scattering: Protocol Validated for Measurements of 60 and 203nm Diameter Nanomaterials Is Now Extended to 100 and 400nm. *Int. J. Pharm.* **2016**, *515* (1–2), 245–253.
- (43) Sadiku, E. R.; Sanderson, R. D. Particle Size and Size Distribution of styrene/sulfopropylmethacrylate/2,2'-azobis[2-Methyl-N-(2-Hydroxyethyl) Propionamide] (styrene/SPM/VA-086) and styrene/N,N-Dimethyl-N-Methacryloxyethyl-N-(3-Sulfopropyl) Ammonium Betain [styrene/SPE/oil-Soluble 1,1-A. *J. Appl. Polym. Sci.* **2006**, *102*, 166–174.
- (44) Cao, A. Light Scattering. Recent Applications. *Anal. Lett.* **2003**, *36* (15), 3185–3225.
- (45) Bartling, C. M.; Andre, J. C.; Howland, C. A.; Hester, M. E.; Cafmeyer, J. T.; Kerr, A.; Petrel, T.; Petrikovics, I.; Rockwood, G. A. Stability Characterization of a Polysorbate 80-Dimethyl Trisulfide Formulation, a Cyanide Antidote Candidate. *Drugs R D* **2016**, *16* (1), 109–127.
- (46) Kiss, L.; Holmes, S.; Chou, C. E.; Dong, X.; Ross, J.; Brown, D.; Mendenhall, B.;

- Coronado, V.; De Silva, D.; Rockwood, G. A.; et al. Method Development for Detecting the Novel Cyanide Antidote Dimethyl Trisulfide from Blood and Brain, and Its Interaction with Blood. *J. Chromatogr. B* **2017**, *1044–1045*, 149–157.
- (47) Harris, D. C. *Quantitative Chemical Analysis*, 6th ed.; Fiorillo, J., Rossignol, R., Byrd, M. L., McCorquodale, A., Eds.; W. H. Freeman and Company: New York, 2003.
- (48) Ancha, M. Screening, Characterization and Formulation of Selected Sulfur Molecules as Potent Antidotes in Cyanide Poisoning., Sam Houston State University, 2012.

APPENDIX

Glossary

CN: cyanide

TS: thiosulfate

NT: nitrite

DMTS: dimethyl trisulfide

DMDS: dimethyl disulfide

poly80: polyoxyethylenesorbitan monooleate

span80: sorbitan monooleate

DMTS-F1: dimethyl trisulfide formulation 1

DMTS-F2: dimethyl trisulfide formulation 2

DS/F1: donor solution prepared by formulation 1

DS/F2: donor solution prepared by formulation 2

BBB: blood brain barrier

IC: ion chromatography

HPLC: high pressure liquid chromatography

DLS: dynamic light scattering

PAMPA: parallel artificial membrane permeability assay

IM: intramuscular

S.D.: sample standard deviation

VITA

Chathuranga Chinthana Hewa Rahinduwage

EDUCATION

- Master of Science student in Chemistry at Sam Houston State University, August 2015 – present. Thesis title: Analytical method development for cyanide antidotes and characterization of a new formulation of dimethyl trisulfide.
- Undergraduate degree (November 2012) in Chemistry at Institute of Chemistry Ceylon, Sri Lanka.

ACADEMIC EMPLOYMENT

- Graduate Teaching Assistant, Department of Chemistry, Sam Houston States University August 2015 – May 2017.
Responsibilities include: assisting labs CHEM 1406 (Inorganic and Environmental Chemistry), CHEM 1412 (General Chemistry 2 Inorganic and Analytical) CHEM 1407 (Introductory Organic and Biochemistry)
- Graduate Research Assistant - Dr. Petrikovics Lab, Department of Chemistry, Sam Houston State University, Huntsville, Texas., August 2015 – Present.
Research activities include characterization of different formulations of potential cyanide antidote molecule, dimethyl trisulfide.
Collaborative work on HPLC method optimization and determination of Vitamin D3 for American Heart Association funded grant-in-aid project, “Sex Differences in Vitamin D During Myocarditis/Dilated Cardiomyopathy (DCM)”, by Dr. DeLisa Fairweather’s group at Mayo Clinic in Jacksonville, FL.

PRESENTATIONS AT PROFESSIONAL MEETINGS

1. **Hewa R., C. C.**; Mendenhall, B.; Ross, M.; Baca, W.; Petrikovics, I.; Kiss, L.; Investigating the Membrane Penetration of a novel Cyanide Antidote (CAX1) in a Blood Brain Barrier model (BBB-PARALLEL ARTIFICIAL MEMBRANE PERMEABILITY ASSAY). Texas Academy of Science, Junction, Texas, March, 2016 (Poster No: 036.162 G).
2. Kiss, L.; Chou, Ch-E.; Mendenhall, B.; Crews, S.R.; Coronado, V.; Lowry, L.; Dong, X.; Hewa R., C. C.; Kaur, M.; Alam, M.N.; Hossain M.S.; Thompson, D.E.; Petrikovics, I. Analytical method developments for the cyanide antidote CAX1 for solubility, pharmacokinetics and blood brain-barrier penetration characterization. 55th SOT Annual Meeting, New Orleans, March, 2016 (Poster No: P611).

3. **Hewa R., C. C.**; Medenhall, B.; Ross, M.; Baka, W.; Petrikovics, I.; Kiss, L. Membrane penetration of dimethyl trisulfide (DMTS) in Parallel Artificial Membrane Permeability Assay (PAMPA), A blood brain barrier model. Woodlands Center Research Symposium, The Woodlands, TX, April, 2016.
4. Kiss, L., Ebrahimpour, A., Hewa R., C.C.; Gaspe Ralalage, R.D., Xinmei Dong, X., Deli, M., Sipos, P., Revesz, P., Thompson, D.E., Rockwood, G.A., Petrikovics. Antidotal Efficacy and Pharmacokinetics of Dimethyl Trisulfide (DMTS) as a Novel Cyanide (CN) Antidote. 20th Biannual Medical Defense Bioscience Review, US Army Medical Research Institute of Chemical Defense, Aberdeen Proving Ground, MD, June, 2016 (Poster Number: 071).
5. **Hewa R., C. C.**; Gaspe Ralalage, R. D.; Ebrahimpour, A.; Petrikovics, I. Determining the Surfactant and Stirring Effects on the Permeability of Dimethyl Trisulfide (DMTS) in the Parallel Artificial Membrane Permeability Assay (PAMPA). ACS SWRM meeting, Galveston, Texas, November, 2016 (Abstract and Poster No: 544).
6. Gaspe Ralalage, R. D.; Hewa R, C. C.; Ebrahimpour, A.; Petrikovics, I. Different Sulfur Donor Efficacy for Cyanide Intoxication *in vitro*. ACS SWRM meeting, Galveston, Texas, November, 2016 (Abstract and Poster No: 498).
7. **Hewa R., C. C.**; Gaspe Ralalage, R. D.; Warnakula, I.K; Preethika D. K. N.; Kiss, L.; Ebrahimpour, A.; Petrikovics, I.; Characterization of the cyanide antidote candidate SAX6 in two formulation forms: Blood Brain Barrier(BBB) penetration, Size distribution, In vivo efficacy and Pharmacokinetics. 56th SOT Annual Meeting, Baltimore, Maryland, March, 2017 (Abstract No: 2052, Poster No: P214).
8. Gaspe Ralalage, R.D.; Hewa R., C. C.; Thompson, D.; Ebrahimpour, A.; Petrikovics, I. Fluorescent detection method for the cyanide antidote SDX6 using a sulfane sulfur probe. 56th SOT Annual Meeting, Baltimore, Maryland, March, 2017 (Abstract No: 2073, Poster No: P235).
9. Gaspe Ralalage, R.D., Hewa R., C.C., Ebrahimpour, A., Petrikovics, I., In vitro sulfur donor reactivity of various cyanide antidote candidates. Texas Academy of Science Annual Meeting, Belton, Texas, March, 2017 (Poster No: 007.006 G).
10. **Hewa R, C. C.**; Gaspe Ralalage, R. D.; Warnakula, I.K.; Ebrahimpour, Afshin; Petrikovics, I. Modelling Blood Brain Barrier (BBB) penetration by *in-vitro* permeability study with the newly formulated cyanide (CN) antidote, dimethyl

- trisulfide (DMTS), Texas Academy of Science Annual Meeting, Belton, Texas, March, 2017 (Oral presentation No: 017.044 G).
11. Kumarasinghe K.D.M.S.P. K., Hewa. R., C. C., Pathiratne K.A.S., De Silva D. S. M. Electrodeposition of CdS thin films using different sulfur sources for CdS/CdTe solar cells. Book of Abstracts: University of Kelaniya Annual Research Symposium, 2014, P118.
 12. Kumarasinghe K.D.M.S.P. K., Hewa. R., C. C., Pathiratne K.A.S., De Silva D. S. M. Electrochemical deposition and characterization of CdTe thin films. Book of Abstracts: University of Kelaniya Annual Research Symposium, 2014, P119.
 13. **Hewa. R., C. C.;** Gunawardhane H.D. Use of *curcuma longa* as a metallochromic indicator for the titration of iron(III) with EDTA, Chemistry in Sri Lanka, 2013, Volume 30, P36.

ACADEMIC AWARDS

- “All-rounder Best Performer Award 2012” Second place for multidisciplinary skills as a student during the period 2009 to 2012 in College of Chemical Sciences, Institute of Chemistry Ceylon, Sri Lanka
- Subject prize for the “Best Performance in Information Technology for Chemistry – 2012” at the level 3 and 4 at Institute of Chemistry Ceylon, Sri Lanka
- Sam Houston State University(SHSU) Chemistry Academic Scholarship – Summer 2016
- SHSU College of Sciences Graduate Summer Scholarship for Thesis Research – Summer 2016
- SHSU College of Arts and Sciences (COAS) Special Award – Fall 2016
- SHSU Graduate Studies Scholarship Award – Fall 2016
- SHSU Graduate Studies Scholarships – Spring 2017
- Award Nominations:
 1. SHSU COSET Student Excellence in Research 2017
 2. SHSU Graduate Student Award by Office of Graduate Studies 2017
 3. SHSU 23rd Annual Sammys Outstanding Graduate Student Leader 2017

PROFESSIONAL MEMBERSHIPS

- Member of Texas Academy of Science (2016 and 2017)
Associate Member of the Institute of Chemistry Ceylon